

23. VOLCANIC ROCKS FROM LEG 67 SITES: MINERALOGY AND GEOCHEMISTRY¹

R. C. Maury,² H. Bougault,³ J. L. Joron,⁴ D. Girard,² M. Treuil,⁴ J. Azéma,⁴ J. Aubouin⁴

ABSTRACT

Mineralogical (microprobe) and geochemical (X-ray fluorescence, neutron activation analyses) data are given for 18 samples of volcanic rocks from the Guatemala Trench area (Deep Sea Drilling Project Leg 67). Typical fresh oceanic tholeiites occur in the trench itself (Hole 500) and in its immediate vicinity on the Cocos Plate (Site 495). Several samples (often reworked) of "spilitic" oceanic tholeiites are also described from the Trench: their mineralogy (greenschist facies association—actinolite + plagioclase + chlorite) and geochemistry (alteration, sometimes linked to manganese and zinc mineralization) are shown to result from high-temperature (300°–475°C) hydrothermal seawater–basalt interactions. The samples studied are depleted in light rare-earth elements (LREE), with the exception of the slightly LREE-enriched basalts from Hole 500. The occurrence of such different oceanic tholeiites in the same area is problematic.

Volcanic rocks from the Guatemala continental slope (Hole 494A) are described as greenschist facies metabasites (actinolite + epidote + chlorite + plagioclase + calcite + quartz), mineralogically different from the spilites exposed on the Costa Rica coastal range (Nicoya Peninsula). Their primary magmatic affinity is uncertain: clinopyroxene and plagioclase compositions, together with titanium and other hydromagnaphile element contents, support an "active margin" affinity. The LREE-depleted patterns encountered in the present case, however, are not frequently found in orogenic samples but are typical of many oceanic tholeiites.

INTRODUCTION

Eighteen samples of volcanic rocks from Leg 67 sites (Holes 494A, 495, 499B, 499C, 499D, 500, 500B) in the Guatemala Trench have been investigated for major and trace element distributions (by X-ray fluorescence and neutron activation analyses) and compositions of primary minerals (by microprobe). The locations of the sites studied are shown on the schematic cross section of Figure 1 (from Aubouin et al., 1979). The basalts from Site 495 represent the upper part of the oceanic crust of the Cocos Plate, off the Trench. Those from Sites 499 and 500 were recovered in the Trench itself; the samples from Holes 499B and 500 are considered *in situ*, and represent the first oceanic crust basalts to be sampled in an active trench; lavas from Holes 499C, 499D, and 500B were only found as pebbles or reworked materials, and their primary position is unknown. Lastly, volcanic rocks of andesitic (*sensu lato*) composition were recovered from the bottom of Hole 494A, on the Guatemala continental slope, just above the assumed subduction place; they are overlaid by an Upper Cretaceous to Pleistocene sedimentary sequence.

The study of Leg 67 volcanic rocks thus allows two major problems to be investigated: (1) the behavior of the oceanic crust in a Pacific trench environment; and (2) the magmatic affinity of volcanic rocks drilled in the immediate vicinity of a subduction place.

LITHOLOGY

Site 494

We studied four core-catcher samples from Hole 494A: 29,CC (0–4 cm), 31,CC (18–20 cm), 33,CC (30–32 cm), and 35,CC (8–10 cm). These contain porphyritic volcanic rocks, characterized by abundant, well-preserved clinopyroxene phenocrysts, some of centimeter size. Plagioclase is present as phenocrysts of smaller size and as microphenocrysts. The groundmass contains primary clinopyroxene and plagioclase microlites, but has largely recrystallized as a "spilitic" mineral assemblage: chlorite + albite + epidote + actinolite + quartz. Calcite is sometimes associated with quartz-filled vesicles and veinlets. Summarizing, these samples are typically greenschist facies metabasites, with well-preserved primary clinopyroxenes and plagioclases.

Site 495

The six samples from Site 495 we studied are: Sample 495-46-1, 138–143 cm, 495-47-1, 3–8 cm, 495-48-1, 19–21 cm, 495-48-2, 123–126 cm, 495-48-4, 82–86 cm, and 495-48-4, 118–123 cm. All are subaphyric basalts with well-preserved primary texture and mineralogy. Plagioclase is the dominant phenocryst; the groundmass is well-crystallized (plagioclase + clinopyroxene + olivine + magnetite). Olivine is lacking as phenocrysts in the two upper samples (495-46-1 and 495-47-1) and present in the others (495-48-1 to 495-48-4), which presumably belong to another magmatic unit.

Sites 499 and 500

Hole 499B is represented by two samples: a well-crystallized subaphyric basalt (499B-10-1, 15–21 cm) with rare plagioclase and clinopyroxene phenocrysts and

¹ Aubouin, J., von Huene, R., et al., *Init. Repts. DSDP*, 67: Washington (U.S. Govt. Printing Office).

² Université de Bretagne Occidentale, Avenue Le Gorgeu, 29283 Brest, France.

³ Centre Océanologique de Bretagne, Plouzané, 29273 Brest, France.

⁴ Université Pierre et Marie Curie, Place Jussieu, 75230 Paris, France.

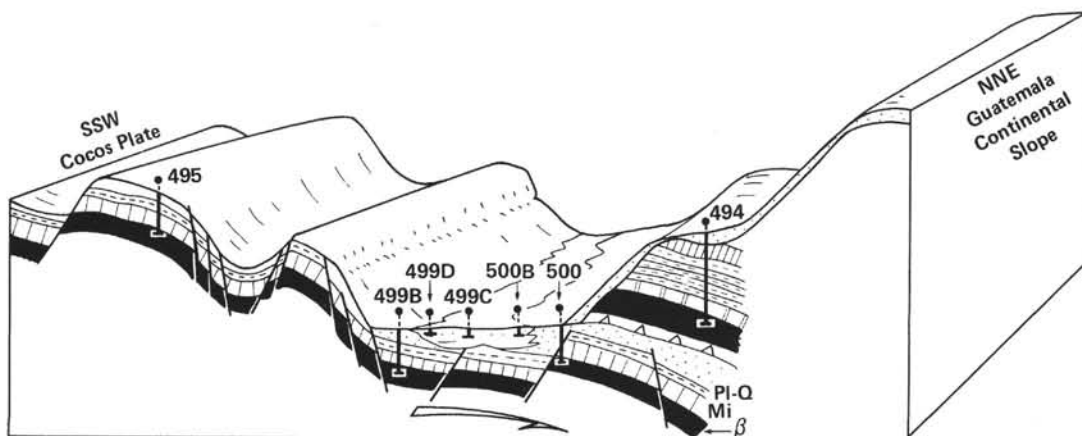


Figure 1. Position of Leg 67 sites (slightly modified from Aubouin et al., 1979). (PI-Q and Mi = Pliocene-Quaternary and Miocene deposits; β = basalts.)

chlorite veinlets in the matrix, and a doleritic coarse-grained basalt (499B-10-140, 46 cm), the groundmass of which has suffered a considerable development of actinolite.

Hole 499C. Two coarse-grained basalt samples (499C-1-1, 3-4 cm and 499C-1-1, 38-43 cm) were recovered from this site. They had largely recrystallized to a greenschist facies mineral association: actinolite + chlorite + albite + opaque oxides. The remaining primary minerals are clinopyroxenes and plagioclases (phenocrysts and microlites).

Hole 499D. Sample 499D-1-1, 33-35 cm shows plagioclase and clinopyroxene phenocrysts and microlites in a chlorite- and albite-rich groundmass.

Hole 500. Samples 500-18-1, 52-54 cm and 500-19-1, 24-28 cm are very well-preserved subaphyric basalts with plagioclase, clinopyroxene, olivine, and spinel in the groundmass and quite rare phenocrysts of olivine, plagioclase, and clinopyroxene. Olivine is altered in Section 500-18-1 and fresh in Section 500-19-1.

Hole 500B. Sample 500B-3-1, 79-88 cm is a coarse-grained basalt very similar to those from Hole 499C. Primary clinopyroxene and plagioclase phenocrysts are dispersed in a groundmass largely recrystallized to chlorite + actinolite + albite, in which pyrite crystals are very abundant.

MAJOR ELEMENT COMPOSITIONS

X-ray fluorescence analyses are presented in Tables 1 to 3.

Site 494, Hole 494A (Table 1)

On the basis of the results at hand, the composition of our samples does not depart very much from the composition of altered oceanic crust basalts. The high values of the loss on ignition are in good agreement with the importance of hydrated phases (chlorite, actinolite) in the metamorphic parageneses of these rocks. SiO_2 contents ranging from 48% to 54.6% are higher than those of most oceanic tholeiites, and the most silica-rich sample (494A-31, CC) falls in the range of "andesitic" lavas. The interpretation of other major element contents

Table 1. Major element compositions (%), Hole 494A.

	Sample (interval in cm)			
	494A-29, CC (0-4)	494A-31, CC (18-20)	494A-33, CC (30-32)	494A-35, CC (8-10)
SiO_2	51.88	54.62	52.94	47.99
TiO_2	0.35	0.50	0.41	0.51
Al_2O_3	14.60	15.43	14.61	14.78
Fe_2O_3	8.05	9.75	7.71	8.54
MnO	0.14	0.27	0.12	0.16
MgO	8.68	5.62	7.95	8.70
CaO	8.43	5.52	3.47	7.30
K_2O	0.47	0.19	0.52	0.45
P_2O_5	0.10	0.06	0.04	0.08
Loss on ignition (110°C)	0.79	0.57	1.33	1.46
Loss on ignition (1050°C)	3.32	3.27	3.96	4.99

Note: Total iron is expressed as Fe_2O_3 .

gives some contradictory information concerning the magmatic affinity of Hole 494A samples: TiO_2 values of 0.35% to 0.5% are compatible with an orogenic magma type, but Al_2O_3 values of 14.6% to 15.4% remain clearly lower than the mean value of Al_2O_3 in andesites; and the K_2O content of 0.2% to 0.5% is close to that of altered oceanic tholeiites and lower than the K_2O values in andesites.

Site 495 (Table 2)

All the major element concentrations fall in the range of typical ocean-floor tholeiites. The upper magmatic unit, Sections 495-46-1 and 495-47-1 is TiO_2 -enriched and MgO - and CaO -depleted, with respect to the lower unit, Section 495-48-2.

Sites 499 and 500 (Table 3)

As, at Site 495, all the compositions encountered are typical of oceanic tholeiites. The samples rich in chlorite and actinolite (Section 499C-1-1) show important loss on ignition (>3.5%). The small number of samples from Holes 499B and 500 precludes identification of separate magmatic units.

Table 2. Major element compositions (%) and C.I.P.W. norms, Site 495.

	Sample (interval in cm)					
	495-46-1, 138-143	495-47-1, 3-8	495-48-1, 19-21	495-48-2, 123-126	495-48-4, 82-86	495-48-4, 118-123
SiO ₂	49.83	50.06	49.98	50.37	50.55	50.68
TiO ₂	1.99	2.02	1.54	1.51	1.50	1.46
Al ₂ O ₃	15.76	16.01	16.07	15.65	15.57	14.82
Fe ₂ O ₃	10.85	10.51	10.37	9.82	9.77	9.95
MnO	0.15	0.17	0.15	0.15	0.15	0.15
MgO	6.05	5.93	6.56	7.37	7.40	7.03
CaO	11.31	11.69	12.33	12.14	12.06	12.07
Na ₂ O	2.64	3.19	2.48	2.34	3.55	3.06
K ₂ O	0.39	0.39	0.28	0.27	0.09	0.28
P ₂ O ₅	0.25	0.31	0.16	0.20	0.16	0.17
Total	99.22	100.28	99.92	99.82	100.80	99.67
Loss on ignition 110°C	1.67	1.62	1.24	1.15	1.11	1.38
Loss on ignition 1050°C	1.34	1.25	1.18	0.99	0.68	1.09
Q	0.80		0.54			
or	2.34	2.32	1.67	1.61	0.53	1.67
ab	22.71	27.15	21.18	19.99	29.68	26.19
an	30.52	28.39	32.20	31.73	26.30	26.19
ne					0.19	
di { wo	10.39	11.65	11.90	11.60	13.57	13.89
en	5.79	6.55	6.80	7.01	8.23	8.22
fs	4.19	4.63	4.58	3.96	4.60	4.98
en	9.53	4.50	9.34	11.52		5.43
fs	6.89	3.18	6.30	6.51		3.29
fo		2.66	0.25		7.15	2.85
fa		2.08	0.18		4.41	1.91
mt	2.40	2.30	2.28	2.15	2.13	2.19
il	3.84	3.86	2.95	2.90	2.85	2.81
ap	0.60	0.74	0.38	0.48	0.38	0.41
S.I.	31.85	30.98	34.89	38.87	37.03	36.11
D.I.	25.85	29.46	22.85	22.15	30.40	27.86

Note: Total iron is expressed as Fe₂O₃; S.I. = Solidification Index; D.I. = Differentiation Index.

MINERALOGY

All the mineral analyses (1-160) presented in this paper have been obtained with a Camebax automated microprobe (Microsonde Ouest, Brest) under the following working conditions: 15 KV, 10-12 nA; counting time: 6 s. The value 0.1% is considered, on the basis of routine analysis, to be the limit of detection, under which the given calculated concentrations are not significant.

Site 494

Magmatic minerals. The only primary minerals chemically well-preserved in Hole 494A samples are clinopyroxenes (Table 4) and plagioclases (Table 5). The clinopyroxenes plot near the limit of the endiopside and augite fields of the Ca-Mg-(Fe + Mn) diagram (Fig. 2A). They are characterized by their high Mg/Fe ratio, high SiO₂ content, low TiO₂ and Al₂O₃, and relatively high Cr₂O₃ (reaching up to 1%). Such magnesio-calcic clinopyroxenes of endiopside composition are relatively uncommon in volcanic rocks: they have been found in some ocean-floor basalts (e.g., North Atlantic, Leg 49; Wood et al., 1979), but the compositions encountered are more Ti-rich than those of Hole 494A pyroxenes. Endiopside has also been found in active-margin basalts (Konda, 1970; Le Guen de Kerneizon et al., 1979). Chromiferous diopside, the composition of which is very similar to that encountered in Site 494 rocks, has been shown to crystallize at an early stage of fractionation in

Table 3. Major element compositions (%) and C.I.P.W. norms, Holes 499B, 499C, 499D, 500, and 500B.

	Sample (interval in cm)							
	499B-10-1, 15-21	499B-10-1, 40-46	499C-1-1, 3-4	499C-1-1, 38-43	499D-1-1, 33-35	500-18-1, 52-54	500-19-1, 24-28	500B-3-1, 79-88
SiO ₂	49.96	48.82	49.89	50.03	50.49	49.80	49.14	50.42
TiO ₂	0.98	0.94	1.38	1.31	0.98	1.81	1.68	1.07
Al ₂ O ₃	14.73	15.39	19.77	18.76	15.42	17.77	16.28	15.16
Fe ₂ O ₃	8.93	9.26	7.93	9.07	9.40	8.78	9.22	9.71
MnO	0.14	0.16	0.31	0.39	0.16	0.12	0.14	0.18
MgO	8.35	8.56	9.34	7.92	8.88	6.23	8.12	8.93
CaO	12.20	12.34	6.39	8.80	12.10	11.71	11.11	12.44
Na ₂ O			3.67	3.49	1.89	3.07	2.37	1.70
K ₂ O	0.10	0.09	0.19	0.16	0.04	0.43	0.65	0.05
P ₂ O ₅	0.09	0.11	0.14	0.09	0.08	0.31	0.29	0.09
Total			99.01	100.02	99.44	100.03	99.00	99.75
Loss on ignition 110°C	0.49	0.38	1.53	1.05	0.28	2.09	1.04	0.21
Loss on ignition 1050°C	1.16	1.20	3.77	2.69	1.02	1.62	0.99	1.25
Q					1.18			1.60
or			1.14	0.95	0.24	2.56	3.91	0.30
ab			31.56	29.74	16.21	26.15	20.41	14.53
an			31.30	35.32	33.94	33.68	32.45	33.95
co			2.29					
di { wo				3.37	11.01	9.51	9.07	11.62
en				2.09	6.95	5.80	5.81	7.29
fs				1.08	3.37	3.17	2.67	3.61
en			15.05	7.69	15.46	4.68	10.18	15.18
fs			5.48	3.97	7.49	2.56	4.68	7.51
fo			6.02	7.07		3.60	3.22	
fa			2.42	4.02		2.17	1.63	
mt			1.75	1.99	2.07	1.93	2.04	2.14
il			2.67	2.51	1.89	3.46	3.25	2.05
ap			0.34	0.22	0.19	0.74	0.70	0.22
S.I.			45.23	39.36	45.71	35.08	41.49	45.55
D.I.			32.71	30.69	17.63	28.71	24.32	16.43

Note: Total iron is expressed as Fe₂O₃; S.I. = Solidification Index; D.I. = Diffraction Index.

Table 4. Clinopyroxenes (in %) from Hole 494A.

Sample 494A-29, CC (0-4 cm)	Analysis No.											
	1	2	3	4	5	6	7	8	9	10	11	12
SiO ₂	50.68	52.83	52.88	51.92	53.13	54.33	52.73	52.58	52.51	53.24	52.17	53.57
TiO ₂	0.33	0.17	0.14	0.14	0.20	0.08	0.15	0.13	0.19	0.24	0.11	0.07
Al ₂ O ₃	6.80	2.94	3.01	3.99	2.53	1.41	3.05	3.70	2.01	1.97	3.63	3.14
Cr ₂ O ₃	0.00	0.22	0.31	0.32	0.18	0.16	0.00	0.00	0.16	0.19	0.26	0.01
FeO	6.49	5.51	5.53	4.76	5.36	5.99	6.59	5.55	6.63	6.86	5.05	4.92
MnO	0.20	0.14	0.16	0.23	0.09	0.20	0.19	0.11	0.11	0.13	0.00	0.14
MgO	16.25	18.29	18.60	16.57	18.32	21.31	16.95	17.80	16.43	17.15	18.16	17.87
CaO	18.64	19.46	18.93	21.58	19.62	16.29	19.54	20.92	20.95	20.89	19.71	20.60
Na ₂ O	0.15	0.13	0.09	0.10	0.08	0.07	0.15	0.14	0.12	0.15	0.09	0.06
K ₂ O	0.00	0.05	0.00	0.00	0.00	0.00	0.00	0.03	0.00	0.02	0.00	0.04
Total	99.54	99.74	99.65	99.61	99.51	99.84	99.35	100.96	99.11	100.84	99.18	100.42
{ Ca	40.12	39.46	38.43	44.47	39.75	32.08	40.36	41.83	42.69	41.61	40.29	41.68
Mg	48.63	51.59	52.55	47.50	51.62	58.40	48.70	49.51	46.59	47.53	51.64	50.31
Fe + Mn	11.25	8.95	9.02	8.03	8.63	9.52	10.93	8.66	10.72	10.86	8.07	8.01
Sample 494A-33, CC (30-32 cm)	13	14	15	16	17	18	19	20	21	22	23	24
SiO ₂	51.58	53.00	52.59	51.51	51.87	53.71	53.55	52.69	51.69	52.76	52.29	62.60
TiO ₂	0.29	0.26	0.32	0.36	0.23	0.19	0.22	0.21	0.24	0.28	0.42	0.30
Al ₂ O ₃	3.67	3.64	3.29	4.02	3.40	1.91	1.62	2.66	3.46	3.27	4.02	2.80
Cr ₂ O ₃	0.96	1.02	0.17	0.18	0.44	0.28	0.33	0.23	0.02	0.20	0.16	0.08
FeO	5.44	4.85	5.90	7.19	4.71	6.11	5.47	6.12	6.73	5.55	7.30	8.07
MnO	0.22	0.16	0.10	0.15	0.26	0.09	0.16	0.05	0.21	0.00	0.30	0.10
MgO	17.88	17.30	17.18	17.08	17.00	19.11	19.57	17.79	17.20	17.55	18.97	18.35
CaO	19.08	20.04	20.86	19.62	20.53	18.49	18.38	20.95	20.89	20.63	16.89	18.51
Na ₂ O	0.15	0.14	0.14	0.18	0.16	0.08	0.02	0.12	0.17	0.08	0.06	0.14
K ₂ O	0.00	0.00	0.01	0.00	0.00	0.03	0.02	0.00	0.00	0.00	0.00	0.00
Total	99.27	100.41	100.56	100.29	98.60	100.00	99.34	100.82	100.61	100.32	100.41	100.95
{ Ca	39.45	41.74	42.19	39.95	42.73	37.05	36.76	41.47	41.58	41.78	34.32	33.51
Mg	51.41	50.10	48.33	48.38	49.20	53.25	54.45	49.00	47.65	49.44	53.61	53.50
Fe + Mn	9.14	8.16	9.48	11.67	8.07	9.70	8.79	9.53	10.78	8.78	12.07	12.99

Note: Analyses numbers 1 to 6 and 13 to 18 are cores of phenocrysts; 7, 8, 19, and 20 are rims of phenocrysts; 9, 10, 20 to 24 are microphenocrysts and 11 and 12 microlites.

Table 5. Hole 494A—analyses of primary plagioclases (25-34) and other minerals (in %).^a

Sample	494A-29, CC (0-4 cm)									
	25	26	27	28	29	30	31	32	33	34
SiO ₂	50.44	51.37	51.64	56.44	50.32	55.87	51.57	49.59	52.95	51.85
TiO ₂	0.00	0.00	0.04	0.05	0.00	0.02	0.00	0.00	0.00	0.06
Al ₂ O ₃	30.71	30.50	30.18	27.62	30.79	27.38	30.48	31.66	28.96	29.74
Cr ₂ O ₃	0.00	0.00	0.00	0.01	0.00	0.00	0.00	0.01	0.00	0.00
FeO	0.86	0.65	1.09	0.73	1.02	0.84	0.91	1.06	0.80	0.73
MnO	0.00	0.00	0.00	0.04	0.00	0.02	0.00	0.16	0.00	0.00
MgO	0.04	0.09	0.10	0.00	0.07	0.02	0.10	0.13	0.07	0.03
CaO	15.21	14.19	13.45	10.01	14.33	10.49	13.69	15.04	13.05	13.55
Na ₂ O	2.92	3.20	3.59	5.43	3.05	5.41	3.46	2.56	4.00	3.74
K ₂ O	0.00	0.04	0.01	0.03	0.04	0.03	0.11	0.04	0.05	0.07
Total	100.18	100.04	100.10	100.36	99.62	100.08	100.32	100.25	99.88	99.77
{ Ca	74.21	70.85	67.40	50.36	72.03	51.64	68.15	76.27	64.11	66.41
{ Na	25.79	28.93	32.52	49.45	27.72	48.20	31.17	23.47	35.57	33.17
K	0.00	0.21	0.08	0.19	0.25	0.18	0.68	0.26	0.32	0.42
Sample	494A-33, CC (30-32 cm) ¹					494A-31, CC (18-20 cm)			494-29, CC (0-2 cm)	
	35	36	37	38	39	40	41	42	43	44
SiO ₂	67.86	68.33	67.51	43.11	28.91	37.82	38.18	29.20	51.40	51.16
TiO ₂	0.00	0.00	0.00	0.00	0.00	0.00	0.21	0.00	0.00	0.05
Al ₂ O ₃	20.03	20.29	20.78	21.68	18.87	25.64	24.72	19.55	2.59	3.84
Cr ₂ O ₃	0.00	0.00	0.06	0.00	0.00	0.01	0.00	0.05	0.00	0.00
FeO	0.23	0.05	0.20	3.84	19.86	10.18	10.22	23.44	15.77	14.62
MnO	0.00	0.00	0.00	0.00	0.33	0.12	0.12	0.81	0.38	0.34
MgO	0.00	0.00	0.00	0.02	19.93	0.00	0.11	17.80	11.34	10.89
CaO	0.24	0.63	0.72	26.85	0.03	24.13	23.85	0.11	13.67	14.36
Na ₂ O	11.87	11.33	11.29	0.06	0.07	0.02	0.00	0.00	0.28	0.36
K ₂ O	0.05	0.06	0.08	0.04	0.03	0.03	0.00	0.11	0.07	0.24
Total	100.28	100.69	100.64	95.60	88.03	97.95	97.41	91.07	95.50	95.86
Ab %	98.62	96.70	96.19			0.365		0.433	0.444	0.435
FM										

Albite: 35, 37; epidote: 38, 40; chlorite: 39, 41; actinolite: 43, 44. Core of phenocrysts: 25 to 29; 35, 36; rims: 30, 31, 37; groundmass plagioclases: 32 to 34; FM = (Fe + Mn)/(Fe + Mn + Mg).

New Hebrides island-arc tholeiites (Marcelot, 1980; G. Marcelot, personal communication, 1981).

Plagioclases have undergone variable degrees of albitization: some of them are nearly pure albite (Analyses 35–37, Table 5); others show well-preserved calcic plagioclase compositions (25–34, Table 5), which plot into the bytownite-labradorite field, as do most feldspars from oceanic tholeiites and active-margin basalts. Their zoning is predominantly of normal type. They contain appreciable amounts of iron (total iron as FeO reaching up to 1%), but their magnesium content is low ($MgO < 0.1\%$) and the calculated concentrations fall in the range of the analytical precision. They differ in that respect from most plagioclases from ocean-floor tholeiites, including samples from Sites 495, 499, and 500 of Leg 67 and from Leg 66 (Joron et al., 1982), in which Mg content is usually significantly higher (Hawkins, 1977). The low MgO content would favor an “active-margin” affinity for Hole 494A rocks.

Metamorphic minerals. Although the aim of this work was not the detailed study of late paragenesis, some analyses of epidote, chlorite (pycnochlorite-type), and actinolite are presented in Table 5; the calcic amphibole found in Hole 494A appears to be a true actinolite, following Leake's (1978) classification.

Magmatic affinity of clinopyroxenes from Site 494. Leterrier et al., (personal communication, 1981) have proposed several chemical diagrams useful in differentiating among calcic clinopyroxenes of various magmatic affinities. Hole 494A clinopyroxenes have been plotted in these diagrams (Fig. 2B and 2C), together with pyroxenes from “typical” oceanic crust (Hole 499B) and pyroxenes from basalts of the coastal ranges of Costa Rica (Santa Elena, Nicoya, and Herradura areas). These basalts (samples supplied by J. Tournon) are considered to belong to the oceanic tholeiite magma type (Galli-Olivier, 1979; Azéma and Tournon, this volume), and their structural position is like that of Site 494 rocks (Site 494 report, this volume). Figure 2B shows that Santa Elena pyroxenes plot in the alkali basalt field of a Ti versus $(Ca + Na)$ diagram, all others being of tholeiitic or calc-alkalic affinities. In Figure 2C, most of Hole 494A pyroxenes plot in the orogenic basalt field, those from Hole 499B and Costa Rica coastal ranges plotting into the nonorogenic basalt field (including oceanic tholeiites and alkali basalts). Thus clinopyroxene compositions can be considered to support an “active-margin basalt” parentage for Site 494 volcanic rocks.

Site 495

On the whole, the mineral composition of Site 495 volcanic rocks is that of typical oceanic tholeiites, showing that oceanic crust can reach the immediate vicinity of an active trench without undergoing any noticeable mineralogical transformation. Olivine and opaque oxides are often altered, as in many ocean-floor samples; clinopyroxenes (Table 6) are relatively iron-rich augites ($Fs\%: 17–30$), which contain important amounts of TiO_2 and Al_2O_3 ; their groundmass pyroxenes (Analyses 49–54, Table 6) are Fe-enriched and Ca-depleted with respect to the microphenocrysts, following a typical tho-

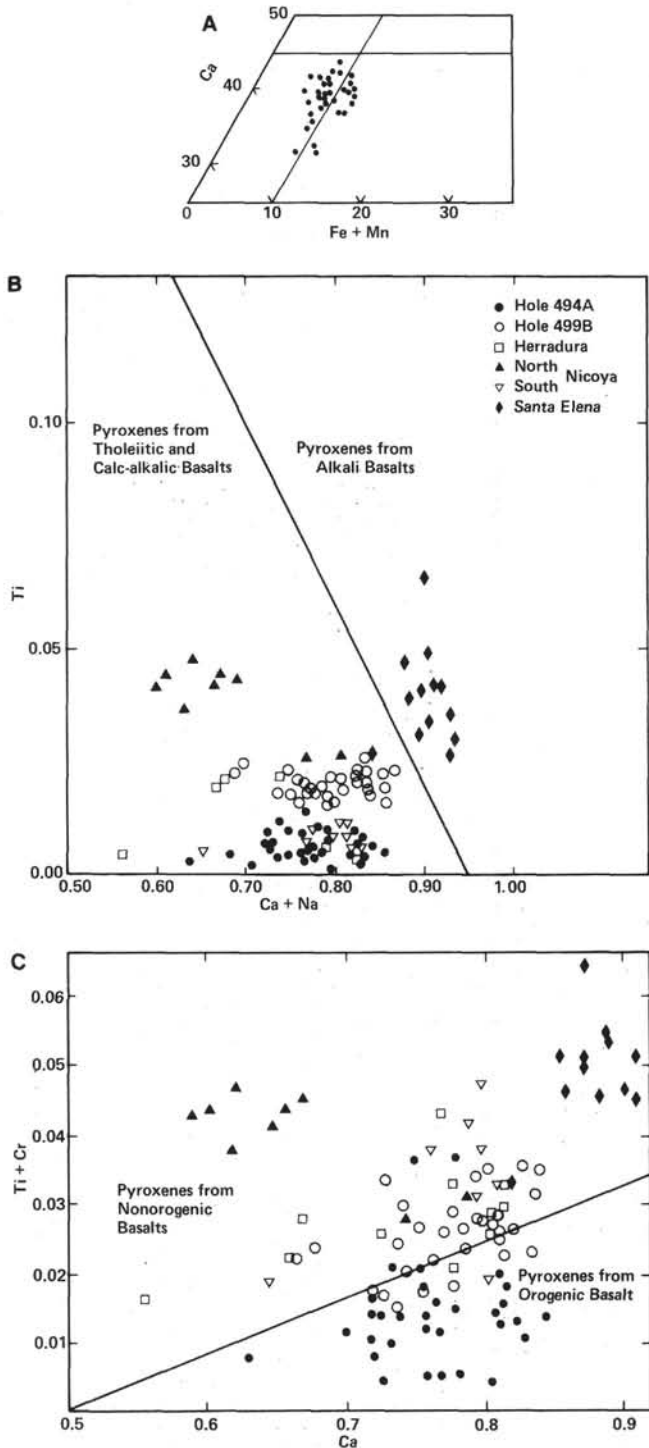


Figure 2. Clinopyroxenes from Hole 494A. A. Position in the Ca-Mg-(Fe + Mn) diagram. B and C. Magmatic parentages. (Diagrams after Leterrier et al., personal communication, 1981; cationic proportions in the structural formulae. Pyroxenes from Hole 494A are compared to those from Hole 499B and those from the volcanic rocks of Herradura, Nicoya, and Santa Elena formations of the Costa Rica coastal ranges; they are considered tholeiites with ocean-floor affinities.)

Table 6. Site 495—pyroxene analyses (in %).^a

Sample Analysis No.	495-46-1, 138-143 cm					495-47-1, 3-8		495-48-4, 118-123 cm		
	45	46	47	48	49	50	51	52	53	54
SiO ₂	45.59	47.69	47.25	47.68	46.89	46.49	43.48	49.09	47.99	46.68
TiO ₂	3.56	2.54	2.80	2.55	3.28	3.17	4.43	1.38	2.35	3.09
Al ₂ O ₃	6.75	4.08	5.60	4.95	4.50	5.52	6.74	4.80	4.95	4.33
Cr ₂ O ₃	0.15	0.04	0.34	0.21	0.00	0.27	0.21	0.30	0.09	0.09
FeO	9.85	10.27	10.32	11.29	16.31	10.56	12.18	10.51	11.53	15.36
MnO	0.23	0.27	0.18	0.26	0.50	0.33	0.31	0.18	0.16	0.47
MgO	11.79	12.65	11.82	11.82	8.36	11.18	9.66	13.76	12.04	9.66
CaO	21.39	20.68	21.34	21.25	19.58	21.21	21.02	19.74	20.55	19.14
Na ₂ O	0.54	0.58	0.56	0.51	0.61	0.55	0.57	0.49	0.66	0.57
K ₂ O	0.00	0.00	0.01	0.02	0.03	0.00	0.00	0.00	0.03	0.00
Total	99.85	98.80	100.22	100.54	100.06	99.28	98.60	100.25	100.35	99.39
{ Ca	46.84	44.48	46.41	45.49	44.17	46.85	47.55	41.80	44.27	42.59
Mg	35.93	37.84	35.77	35.20	26.23	34.36	30.39	40.53	36.07	29.91
Fe + Mn	17.23	17.68	17.82	19.31	29.60	18.79	22.06	17.67	19.66	27.50

^a Microphenocrysts: 45, 47 (cores), 46, 48 (corresponding rims); groundmass pyroxenes: 49 to 54.

leitic trend of evolution (Fig. 3). The feldspars (Table 7) are normally zoned bytownite phenocrysts and labradorite microlites. Their K₂O content is very low (<0.06%), and their MgO content appreciable (up to 0.4%), as in typical ocean-floor basalts. Again, these feldspars are clearly different from those of Site 494. Albited plagioclases have never been found.

Sites 499 and 500 (Holes 499B, 499C, 499D, 500, and 500B)

The mineralogy of samples from these holes is characteristically that of oceanic tholeites, however, the holes show important differences in their major element compositions. Some samples are very fresh (Hole 500), others show variable extents of development of hydrothermal-metamorphic parageneses characterized by the association actinolite + chlorite + albite + quartz + calcite (499B, 499C, 499D, 500B). Among the latter, only one sample from Hole 499B (499B-10-1, 40–46 cm) has been considered as *in situ* by the Shipboard team. Lastly, a few samples (499C-1-1, 38–43 cm; 500B-3-1, 79–88 cm) contain manganiferous ilmenite and/or pyrophanite (MnTiO₃), proving that they have undergone manga-

nese mineralization. Pyrite is common in Section 500B-3-1.

Olivines have only been preserved in the rocks drilled at Hole 500 (Table 8). They show a progressive iron-enrichment (Fa₁₂–Fa₁₈) from the cores to the rims of phenocrysts and to the groundmass crystals.

Clinopyroxenes show important variations from one hole to another (Table 9). A striking difference appears between Hole 500 pyroxenes (Samples 500-18-1, 52–54 cm and 500-19-1, 24–28 cm) and those from other holes. Hole 500 pyroxenes (Analyses 97–104, Table 9) are clearly depleted in silica and enriched in TiO₂, Al₂O₃, CaO, and Na₂O, compared with the other analyses. Their TiO₂ content of 3% to 5% is especially high, comparable to that of clinopyroxenes from the titanium-rich alkali basalts of the Polynesian oceanic islands (Tracy and Robinson, 1977; Brousse and Maury, in press); substitution of the CaTiAl₂O₆ component plays an essential role in their chemistry. Even if quench trend effects (Smith and Lindsley, 1971) have enhanced their Ti and Al^{IV} contents (Mevel and Velde, 1976), all of them being groundmass pyroxenes, it remains undeniable that their chemical composition indicates an “alkalic” tendency

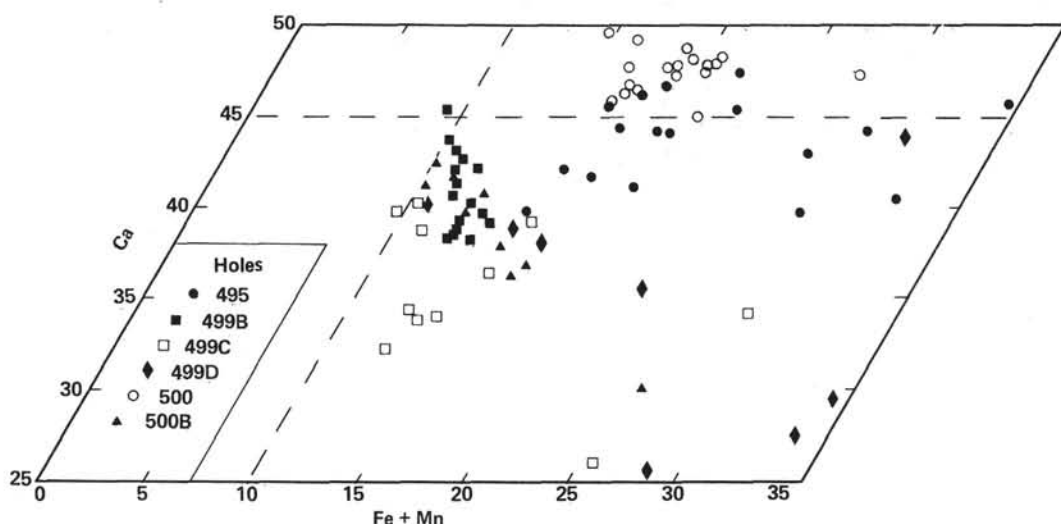


Figure 3. Plot of clinopyroxenes from Sites 495, 499, and 500 in the Ca-Mg-(Fe + Mn) diagram. (The calcic [“alkalic”] character of the salites from Site 500 is stressed.)

Table 7. Site 495: plagioclase analyses (in %).^a

Sample	495-46-1, 138-143 cm						495-47-1, 3-8 cm				495-48-4, 118-123 cm					
	55	56	57	58	59	60	61	62	63	64	65	66	67	68	69	70
SiO ₂	47.96	49.57	49.77	53.82	52.77	54.35	46.98	49.44	52.81	52.65	48.77	48.14	47.82	53.23	50.86	52.79
TiO ₂	0.00	0.00	0.02	0.09	0.08	0.14	0.00	0.08	0.00	0.09	0.00	0.00	0.00	0.03	0.05	0.00
Al ₂ O ₃	32.53	31.77	31.52	28.47	29.56	28.12	33.38	31.51	28.89	29.65	32.43	32.65	32.42	28.51	29.45	28.34
Cr ₂ O ₃	0.00	0.08	0.00	0.00	0.13	0.00	0.00	0.08	0.00	0.00	0.08	0.00	0.00	0.00	0.00	0.09
FeO	0.36	0.55	0.41	0.64	0.73	0.82	0.36	0.12	0.54	0.47	0.31	0.23	0.47	0.61	0.65	0.71
MnO	0.00	0.14	0.00	0.00	0.02	0.00	0.00	0.09	0.02	0.01	0.14	0.01	0.00	0.10	0.00	0.05
MgO	0.18	0.22	0.20	0.22	0.26	0.17	0.18	0.24	0.27	0.22	0.12	0.21	0.16	0.34	0.29	0.39
CaO	16.39	15.64	15.63	12.06	12.81	11.67	17.44	15.07	12.70	13.60	16.37	16.07	17.11	12.91	14.15	13.02
Na ₂ O	2.39	2.82	2.91	4.76	4.13	5.05	1.72	2.96	4.45	4.17	2.42	2.47	2.13	4.44	3.94	4.50
K ₂ O	0.00	0.05	0.01	0.03	0.00	0.06	0.01	0.05	0.04	0.00	0.00	0.00	0.00	0.02	0.00	0.03
Total	99.81	100.84	100.47	100.09	100.49	100.38	100.07	99.64	99.72	100.86	100.64	99.78	100.11	100.19	99.39	99.92
{ Ca	79.15	75.15	74.74	58.21	63.16	55.90	84.80	73.55	61.07	64.29	78.92	78.21	81.52	61.57	66.51	61.43
Na	20.85	24.54	25.19	41.62	36.84	43.78	15.16	26.16	38.73	35.68	21.08	21.79	18.42	38.30	33.49	38.40
K	0.00	0.31	0.07	0.17	0.00	0.32	0.04	0.29	0.20	0.03	0.00	0.00	0.13	0.00	0.17	

^a Core-to-rims compositional variations of phenocrysts: 55 to 58 (250 µm large), 61 to 63 (400 µm large), 65 to 68 (400 µm large). Groundmass plagioclases: 59, 60, 64, 69, 70.

Table 8. Site 500: olivine analyses (in %).^a

Sample	500-19-1, 24-28 cm							
	71	72	73	74	75	76	77	78
SiO ₂	40.36	39.60	40.00	40.32	39.96	39.99	39.84	39.72
TiO ₂	0.02	0.04	0.00	0.00	0.02	0.00	0.04	0.00
Al ₂ O ₃	0.06	0.06	0.04	0.00	0.06	0.04	0.06	0.01
Cr ₂ O ₃	0.00	0.06	0.00	0.06	0.10	0.02	0.04	0.05
FeO	11.80	15.63	11.66	13.36	12.90	14.25	14.31	16.18
MnO	0.06	0.24	0.17	0.08	0.00	0.25	0.19	0.37
MgO	47.82	44.23	47.53	46.82	45.77	45.86	45.58	43.55
CaO	0.26	0.30	0.22	0.28	0.37	0.31	0.33	0.36
Na ₂ O	0.00	0.01	0.00	0.00	0.01	0.04	0.00	0.01
K ₂ O	0.00	0.00	0.00	0.00	0.00	0.00	0.00	0.05
Total	100.38	100.17	99.62	100.92	99.19	100.76	100.39	100.30
Fa %	12.21	16.77	12.26	13.88	13.66	15.07	15.14	17.58

^a Cores of phenocrysts (100 µm large): 71 and 73; corresponding rims: 72 and 74; groundmass olivines: 75 to 78.

of the host magma. This is further shown in Figure 3, where Site 500 pyroxenes plot in the salite field of the Ca – Mg – (Fe + Mn) diagram, all others being augites. The "alkalic" tendency of these pyroxenes, compatible with all their chemical characteristics (Schweitzer et al., 1979), is in excellent agreement with the light REE-enriched pattern of the whole rocks (see the material that follows). Pyroxenes from other sites do not depart from their usual composition in oceanic tholeiites; some samples show restricted compositional variations (e.g., Section 499B-10-1), others are much more scattered in the Ca – Mg – (Fe + Mn) diagram (499C, 499D, 500B).

Feldspars (Table 10) range from primary calcic plagioclase compositions (Sections 500-18-1, 500-19-1), with all the chemical characteristics of oceanic tholeiites (K₂O very low, MgO significant), to almost completely albited feldspars (e.g., Analysis 130, Sample 499C-1-1, 38–43 cm; Analysis 147, Section 500B-3-1). In a given rock (e.g., Sample 499C-1-1, 38–43 cm), progressive compositional variations can be found among the phenocrysts, the normal type zoning of each individual crystal being preserved: An₇₉ to An₆₈ (Analyses 118–121), An₆₁ to An₄₆ (Analyses 122–125), An₄₄ to An₃₃ (Analyses 126–129). This pattern of progressive albitionization is compatible with the high-temperature water-basalt reaction pro-

posed for Hole 499C in the next section on the basis of geochemical considerations.

A magnesiochromite crystal similar to that described in fresh ocean-floor basalts (Sigurdsson and Schilling, 1976; Bougault et al., 1982; Joron et al., 1982) was found in Sample 499B-10-1, 40–46 cm (Analysis 148). (Table 11).

Samples 499C-1-1, 38–43 cm and 500B-3-1, 79–88 cm contain manganiferous oxides (Mn, Fe) TiO₃ ranging in composition from manganiferous ilmenite to pyrophanite (Mn > Fe) (Analyses 151, 152, 153, 154, 159). They are generally represented by small opaque grains in the groundmass, but may appear as larger crystals (Analyses 152, 153) in which Mn and Fe concentrations are variable. Pyrophanite occurs mainly in manganese ores, and Mn-enriched magmatic ilmenite is only observed in the most differentiated rocks of volcanic series (Maury et al., 1980). The origin of the manganiferous oxides in Holes 499C and 500B can thus be ascribed to a postmagmatic stage of mineralization.

Actinolite has been found in basalts of the oceanic crust at the bottom of Hole 499B (Sample 499B-10-1, 40–46 cm: Analyses 149, 150) and in reworked volcanics from Hole 499C (Analysis 155). Chlorite (pycnochlorite-type) is widespread in samples from Holes 499C, 499D, and 500B (Analyses 156, 157, 158, 160). The clayey brownish minerals developed in these holes were not studied in the course of our research.

TRACE ELEMENTS

Analytical Method and Results

Trace element data are presented in Table 12. Data for Hole 487, Leg 66 are presented in the same table because this site is located to the north (15°50'N) in a position similar to those of Sites 495 or 499, with respect to the Middle America Trench. The elements are arranged in the order of increasing atomic numbers. The concentrations of Ti, Mn, and Fe, although not trace elements, have been converted into parts per million (ppm) to present in the same table all the available data

Table 9. Sites 499 and 500: pyroxene analyses (in %).^a

Sample	499B-10-1, 40-46 cm								499C-1-1, 38-43 cm		
	79	80	81	82	83	84	85	86	87	88	89
SiO ₂	51.11	52.66	51.75	51.96	51.64	52.02	51.76	51.79	51.63	52.26	51.85
TiO ₂	0.78	0.51	0.56	0.57	0.76	0.62	0.59	0.76	0.63	0.55	0.65
Al ₂ O ₃	4.91	2.25	3.59	2.35	3.99	3.19	3.02	2.89	3.42	3.09	2.61
Cr ₂ O ₃	0.44	0.00	0.33	0.00	0.41	0.30	0.00	0.10	0.46	0.19	0.07
FeO	5.56	8.48	6.92	9.59	6.06	7.14	8.52	7.50	5.94	6.47	8.87
MnO	0.00	0.26	0.18	0.29	0.09	0.13	0.17	0.26	0.21	0.12	0.23
MgO	15.48	16.83	16.74	16.53	16.00	16.39	16.42	15.85	17.79	17.40	16.82
CaO	21.52	18.72	19.73	18.43	21.31	20.07	19.21	20.67	19.61	19.68	18.90
Na ₂ O	0.30	0.30	0.25	0.28	0.30	0.28	0.26	0.26	0.26	0.24	0.25
K ₂ O	0.02	0.00	0.00	0.00	0.00	0.00	0.07	0.00	0.03	0.00	0.00
Total	100.12	100.01	100.05	100.00	100.56	100.14	100.02	100.08	99.98	100.00	100.25
Ca	45.40	38.23	40.63	37.51	44.06	41.35	39.33	42.37	39.88	40.12	38.26
Mg	45.44	47.83	47.95	46.79	46.01	46.97	46.78	45.21	50.35	49.37	47.36
Fe + Mn	9.16	13.94	11.42	15.70	9.93	11.68	13.89	12.41	9.77	10.50	14.38
Sample	499C-1-1, 38-43 cm			499D-1-1, 33-35 cm			500-18-1, 52-54 cm				
	90	91	92	93	94	95	96	97	98	99	100
SiO ₂	50.64	53.53	51.42	51.53	50.93	50.81	50.83	45.04	44.87	45.39	46.43
TiO ₂	0.91	0.42	0.83	0.87	0.94	0.95	0.98	5.01	4.16	3.93	3.37
Al ₂ O ₃	1.89	1.41	2.34	2.47	1.71	2.02	1.40	5.32	7.30	6.07	6.64
Cr ₂ O ₃	0.00	0.12	0.00	0.87	0.94	0.12	0.00	0.00	0.09	0.16	0.13
FeO	14.55	8.40	10.00	10.44	16.85	13.61	20.68	10.44	10.42	11.49	9.73
MnO	0.35	0.32	0.18	0.27	0.43	0.42	0.40	0.15	0.21	0.30	0.20
MgO	14.46	19.29	15.67	16.23	16.16	14.02	13.03	11.23	10.61	9.79	11.97
CaO	16.68	17.26	19.17	17.50	12.14	16.94	13.15	20.48	21.50	21.25	21.00
Na ₂ O	0.33	0.21	0.28	0.24	0.16	0.35	0.24	0.98	0.57	0.69	0.50
K ₂ O	0.00	0.02	0.00	0.05	0.00	0.00	0.01	0.00	0.00	0.03	0.02
Total	99.81	100.98	99.89	100.47	100.26	99.24	100.72	98.65	99.73	99.10	99.99
Ca	34.44	33.91	39.18	36.13	25.23	35.74	27.54	46.16	46.25	48.22	46.25
Mg	41.54	52.71	44.56	46.60	46.72	41.14	37.98	35.22	36.66	30.90	36.67
Fe + Mn	24.02	13.38	16.26	17.27	28.05	23.12	34.48	18.63	27.08	20.88	17.08
Sample	500-19-1, 24-28 cm				500B-3-1, 79-88 cm						
	101	102	103	104	105	106	107	108	109	110	111
SiO ₂	46.66	44.53	44.54	43.39	50.79	51.16	51.00	51.52	51.42	51.48	50.61
TiO ₂	2.89	3.80	3.88	4.88	1.00	0.83	0.77	0.73	0.79	0.85	0.89
Al ₂ O ₃	6.79	6.56	7.00	6.69	4.47	2.92	4.22	4.30	3.26	2.81	2.33
Cr ₂ O ₃	0.01	0.20	0.16	0.00	0.21	0.02	0.64	0.31	0.22	0.00	0.00
FeO	9.75	12.10	12.12	15.70	7.95	10.31	6.06	6.06	9.09	10.25	15.66
MnO	0.32	0.25	0.31	0.44	0.21	0.14	0.08	0.19	0.23	0.16	0.47
MgO	11.49	10.98	10.09	7.86	15.70	16.41	16.24	16.31	16.23	16.61	15.29
CaO	21.28	20.37	21.36	21.03	19.52	17.50	19.49	20.09	18.21	16.21	14.64
Na ₂ O	0.53	0.66	0.53	0.59	0.27	0.31	0.25	0.20	0.25	0.25	0.24
K ₂ O	0.01	0.06	0.02	0.01	0.00	0.00	0.00	0.00	0.00	0.00	0.00
Total	99.73	99.51	100.01	100.59	100.12	99.60	98.75	99.71	99.70	98.62	100.13
Ca	47.16	44.97	47.35	47.19	40.90	36.10	41.57	42.15	37.89	34.16	30.18
Mg	35.42	33.74	31.13	24.54	45.76	47.09	48.21	47.61	46.97	48.70	43.86
Fe + Mn	17.42	21.30	21.52	28.27	13.34	16.81	10.22	10.24	15.14	17.14	25.96

^a Cores of phenocrysts: 79, 81, 83, 87, 89, 93, 105, 107. Corresponding rims: 80, 82, 84, 88, 90, 94, 106, 108. Ground-mass pyroxenes: 85, 86, 91, 92, 95 to 104, 109, 110, 111.

regarding elements of the first transition series. All the concentrations were determined by X-ray fluorescence (XRF) up to Nb, except Sc (determined by neutron activation analysis—NAA) and Co and Ni (for which both XRF and NAA data are available). From Sb to U, all concentrations were obtained by NAA. For XRF determinations, matrix and instrumental effects were calculated according to the procedures described by Bougault et al., (1977). For NAA, the use of epithermal neutrons strongly diminishes the interferences of ⁴⁶Sc and ⁵⁵Fe. Irradiation is performed in Cd vials; measurements are made with a Ge-Li detector from four days to one month after irradiation (Jaffreziec et al., 1977).

The three samples from Leg 66, Hole 487 are almost identical and are part of the same basaltic unit (Joron et al., 1981); the significant differences observed for alkali metals are discussed farther on. For Site 495, the trace element data clearly show two units; one is represented by two sections (495-46-1, 495-47-1) and the other by

four samples in Core 48. The two samples of Hole 499C are of similar composition and the two samples of Hole 500 are almost identical. Only one sample is available from Hole 499D and one from Hole 500B.

Alteration

Oceanic tholeiites are characterized by low alkali-metal content. The variations of alkali metals in these rocks must be interpreted very carefully in terms of magma genesis. The levels of concentrations of these elements in fresh oceanic tholeiites are approximately as follows: Cs ≈ 0.02 ppm, Rb = 1 ppm, K₂O ≈ 0.1%. Because of these low levels of concentrations, the content of these elements in oceanic basalts is very sensitive to weathering by seawater (Hart, 1969). The uptake of these elements is evident in the case of strong alteration (e.g., Leg 51, Sites 417, 418, at 110 m.y., Donnelly et al., 1979; Bougault et al., 1979; Joron et al., 1980); the Rb concentrations, for example, pass from about 1 ppm for

Table 10. Sites 499 and 500: feldspar analyses (in %).^a

Sample	499B-10-1, 40-46 cm						499C-1-1, 38-43 cm					
Analysis No.	112	113	114	115	116	117	118	119	120	121	122	123
SiO ₂	50.49	53.00	51.70	57.55	53.54	52.90	48.67	52.76	51.05	51.23	52.44	53.57
TiO ₂	0.01	0.04	0.00	0.06	0.03	0.04	0.00	0.00	0.00	0.00	0.10	0.08
Al ₂ O ₃	30.68	29.40	30.62	26.29	29.21	29.27	32.23	29.10	29.86	30.38	29.67	28.82
Cr ₂ O ₃	0.00	0.08	0.00	0.00	0.08	0.00	0.00	0.00	0.00	0.00	0.00	0.00
FeO	0.46	0.68	0.47	0.88	0.65	0.88	0.28	0.61	0.37	0.53	0.50	0.79
MnO	0.07	0.00	0.00	0.00	0.00	0.00	0.00	0.00	0.00	0.00	0.00	0.00
MgO	0.25	0.23	0.31	0.12	0.16	0.18	0.22	0.11	0.25	0.19	0.17	0.13
CaO	14.81	12.79	14.24	9.15	12.38	12.60	15.87	12.15	13.38	13.60	12.38	11.44
Na ₂ O	3.20	4.30	3.50	6.40	4.77	4.41	2.39	4.36	3.72	3.59	4.29	4.69
K ₂ O	0.01	0.03	0.05	0.04	0.00	0.00	0.00	0.00	0.04	0.00	0.00	0.00
Total	99.98	100.55	100.89	100.49	100.82	100.28	99.66	99.09	98.67	99.52	99.55	99.52
{ Ca	71.83	62.08	69.05	44.02	58.93	61.22	78.58	60.63	66.35	67.68	61.47	57.43
Na	28.12	37.73	30.67	55.78	41.07	38.78	21.42	39.37	33.43	32.32	38.53	42.57
K	0.05	0.19	0.28	0.20	0.00	0.00	0.00	0.00	0.22	0.00	0.00	0.00
Sample	499C-1-1, 38-43 cm						499D-1-1, 33-35 cm					
Analysis No.	124	125	126	127	128	129	130	131	132	133	134	135
SiO ₂	54.35	56.58	58.08	57.61	58.89	60.86	63.61	53.83	56.99	53.90	51.44	59.16
TiO ₂	0.07	0.11	0.08	0.11	0.02	0.07	0.01	0.09	0.06	0.06	0.04	0.06
Al ₂ O ₃	28.20	26.82	26.07	26.04	24.84	24.19	23.31	28.58	26.59	28.50	30.22	25.65
Cr ₂ O ₃	0.00	0.02	0.02	0.09	0.00	0.00	0.02	0.00	0.04	0.00	0.02	0.06
FeO	0.60	0.83	0.73	0.71	0.66	0.63	0.25	0.72	0.74	0.61	0.66	0.61
MnO	0.00	0.03	0.00	0.00	0.00	0.12	0.00	0.00	0.00	0.00	0.00	0.01
MgO	0.11	0.07	0.06	0.04	0.09	0.00	0.00	0.31	0.07	0.14	0.22	0.00
CaO	11.08	9.38	9.01	8.72	7.80	6.58	4.09	11.52	9.20	11.34	13.11	7.83
Na ₂ O	5.11	6.05	6.35	6.64	6.99	7.39	9.11	4.71	5.98	4.86	3.43	6.99
K ₂ O	0.00	0.07	0.01	0.08	0.01	0.00	0.04	0.00	0.02	0.00	0.00	0.02
Total	99.52	99.96	100.41	100.04	99.30	99.84	100.44	99.76	99.69	99.41	99.14	100.39
{ Ca	54.52	45.95	43.92	41.87	38.13	32.96	19.84	57.49	45.89	56.30	67.88	38.21
Na	45.48	53.65	56.05	57.69	61.83	67.04	79.92	42.51	53.98	43.69	32.12	61.65
K	0.00	0.40	0.03	0.44	0.04	0.00	0.24	0.00	0.13	0.01	0.00	0.14
Sample	500-18-1, 52-54 cm						500-19-1, 24-28 cm					
Analysis No.	136	137	138	139	140	141	142	143	144	145	146	147
SiO ₂	51.07	50.04	54.05	51.39	50.75	52.99	52.90	52.61	54.37	51.97	58.40	65.58
TiO ₂	0.00	0.09	0.03	0.02	0.03	0.08	0.13	0.09	0.12	0.00	0.04	0.00
Al ₂ O ₃	30.78	32.09	28.34	30.79	31.41	28.79	27.39	29.36	28.07	28.99	25.78	23.12
Cr ₂ O ₃	0.00	0.01	0.04	0.03	0.00	0.00	0.04	0.00	0.07	0.00	0.00	0.00
FeO	0.28	0.45	0.68	0.32	0.26	0.89	2.57	0.70	0.67	0.57	0.99	0.23
MnO	0.00	0.00	0.00	0.00	0.00	0.00	0.00	0.00	0.00	0.05	0.00	0.00
MgO	13.75	0.22	0.15	0.20	0.21	0.32	0.62	0.21	0.12	0.22	0.04	0.07
CaO	13.75	14.70	11.29	13.56	14.92	12.46	11.11	12.81	11.19	12.73	8.65	3.41
Na ₂ O	3.42	3.00	5.03	3.69	3.17	4.44	4.19	4.32	4.86	3.91	6.47	8.99
K ₂ O	0.22	0.08	0.37	0.19	0.13	0.22	0.64	0.17	0.01	0.00	0.09	0.01
Total	99.81	100.68	99.98	100.19	100.88	100.19	99.59	100.27	99.48	98.44	100.46	101.41
{ Ca	68.06	72.67	54.21	66.26	71.71	59.99	57.11	61.52	55.95	64.26	42.26	17.31
Na	30.63	26.84	43.68	32.64	27.56	38.73	38.99	37.50	44.01	35.74	57.20	82.65
K	1.31	0.49	2.11	1.10	0.73	1.28	3.90	0.98	0.04	0.00	0.54	0.04

^a Core-to-rim compositional variations of phenocrysts: 112-113, 114-115, 118-121, 122-125, 126-129, 136-138, 140-141. Groundmass plagioclases: 116, 117, 130-132, 133-135, 139, 142-147.

Table 11. Sites 499 and 500: analyses of manganiferous ilmenite and pyrophanite, magnesiochromite, actinolite, and chlorite (in %).^a

Sample	499B-10-1, 40-46 cm						499C-1-1, 38-43 cm						499D-1-1, 33-35 cm		500B-3-1, 79-88 cm	
Analysis No.	148	149	150	151	152	153	154	155	156	157	158	159	160	159	160	
SiO ₂	0.09	52.46	52.48	0.24	0.26	1.76	1.12	51.84	30.00	29.45	28.11	1.92	30.77			
TiO ₂	0.53	0.18	0.25	50.52	50.98	48.91	50.07	0.34	0.00	0.04	0.00	49.79	0.00			
Al ₂ O ₃	23.45	2.66	3.06	0.00	0.00	0.36	0.07	2.16	16.92	16.25	17.37	0.09	16.67			
Cr ₂ O ₃	37.62	0.01	0.04	0.08	0.02	0.00	0.02	0.00	0.00	0.00	0.00	0.00	0.00	0.00	0.06	
FeO	22.23	15.05	18.62	25.82	29.77	27.39	25.74	18.70	20.49	19.61	23.63	37.64	18.26			
MnO	0.17	0.44	0.29	23.48	18.57	19.61	21.11	0.32	0.20	0.24	0.27	7.39	0.32			
MgO	13.03	14.42	14.33	0.03	0.06	0.00	0.00	12.33	20.15	19.19	18.34	0.12	21.31			
CaO	0.25	12.86	7.41	0.21	0.47	1.34	1.26	10.10	0.18	0.21	0.07	1.36	0.09			
Na ₂ O	0.03	0.65	0.84	0.00	0.02	0.09	0.00	0.42	0.07	0.11	0.00	0.03	0.01			
K ₂ O	0.00	0.05	0.03	0.00	0.02	0.00	0.00	0.01	0.00	0.07	0.04	0.00	0.12			
Total	97.40	98.78	97.35	100.38	100.17	99.06	98.27	97.22	88.01	85.17	87.83	98.34	87.61			
FM		0.376	0.425					0.464	0.366	0.367	0.422		0.329			

^a Magnesiochromite: 148; manganiferous ilmenite and pyrophanite: 151 and 152 (crystal 100 μm large), 153, 154, 159 (groundmass); actinolite: 149, 150 (in patches), 155 (fibrous); chlorite: 156, 157, 158, 160.

Table 12. Trace element data, Holes 487 (Leg 66) and 495, 499C, 499D, 500, 500B (Leg 67).

Sample (interval cm)	Trace Elements (ppm)													
	Sc (NA)	Ti (XRF)	V (XRF)	Cr (XRF)	Mn (XRF)	Fe (XRF)	Co (XRF)	Na	Ni (XRF)	Na	Zn (XRF)	Rb (XRF)	Sr (XRF)	
487-20-1, 55-58	34.0	5040	236	451	1084	70605	44	45	138	144	62	0.4	54	
487-20-1, 72-78	33.9	5160	255	461	1239	73553	45	45	119	127	61	4.9	56	
487-20-1, 82-89	33.4	5040	237	447	1084	68098	46	46	129	136	60	3.1	56	
495-46-1, 138-143	40.1	11940	274	252	1161	79965	39	37.5	92	88	76	7	122	
495-47-1, 3-8	40.0	12120	300	267	1316	77459	39	38.0	82	87	80	8	175	
495-48-1, 17-21	39.8	9240	290	353	1161	76427	41	41.5	99	106	74	4	121	
495-48-2, 123-126	39.5	9060	267	340	1161	72374	43	41.0	104	117	72	3	116	
495-48-4, 82-86	39.0	9000	268	340	1161	72005	40	41.3	105	114	66	0	115	
495-48-4, 118-123	39.1	8760	277	353	1161	73332	42	41.9	107	118	71	5	131	
499C-1-1, 3-4	37.2	8280	235	355	2400	58444	29	28.9	101	93	384	1.1	112	
499C-1-1, 38-43	36.5	7860	238	310	3020	66846	32	31.4	89	95	324	1.8	109	
499D-1-1, 33-35	36.3	5880	220	372	1239	69278	46	44.5	107	111	46	0.5	87	
500-18-1, 52-54	33.2	10860	282	323	929	64709	41	39	112	132	64	3.9	262	
500-19-1, 24-28	33.4	10080	246	304	1084	67952	37	38	128	155	57	6.5	231	
500B-3-1, 79-88	37.7	6420	246	390	1394	71563	41	40	88	95	54	0.4	80	
	Y (XRF)	Zr (XRF)	Nb (XRF)	Sb (NA)	Cs (NA)	Ba (NA)	La (NA)	Ce (NA)	Eu (NA)	Tb (NA)	Hf (NA)	Ta (NA)	Th (NA)	U (NA)
487-20-1, 55-58	26	48	0.3	0.03	0.12	52	0.75		0.81	0.47	1.07	0.033	0.013	
487-20-1, 72-78	27	56	0.6	0.20	0.18		0.80		0.72	0.48	1.17	0.029	0.022	
487-20-1, 82-89	26	44	0.4	0.08	0.12		0.83	1.6	0.66	0.43	1.16	0.028	0.042	
495-46-1, 138-143	54	189	6.7	0.06	0.50	0	7.60	16.8	1.72	1.02	4.6	0.450	0.400	
495-47-1, 3-8	55	201	6.4	0.08	0.41	23	7.40		1.87	1.02	4.3	0.470	0.420	0.08
495-48-1, 17-21	57	122	1.3	0.14	0.18		3.50	8.7	1.40	0.80	2.8	0.140	0.127	
495-48-2, 123-126	44	115	2.6	0.02	0.25		3.40	8.5	1.30	0.80	3.0	0.150	0.113	
495-48-4, 82-86	44	119	2.9	0.01	0.02		3.30		1.42	0.81	2.7	0.150	0.111	
495-48-4, 118-123	44	120	2.2	0.02	0.22	2	3.20	9.8	1.35	0.78	2.9	0.140	0.130	
499C-1-1, 3-4	46	83	1.3	0.27	0.02	6	2.51		1.80	0.75	2.04	0.074	0.047	
499C-1-1, 38-43	37	80	2.0	0.27	0.03		1.98		1.30	0.64	2.00	0.064	0.076	
499D-1-1, 33-35	31	68	0.3				1.45		0.99	0.55	1.46	0.044	0.037	
500-18-1, 52-54	39	141	16	0.17	0.06	35	10.1		1.58	0.75	3.40	1.150	1.090	0.26
500-19-1, 24-28	37	143	14	0.03	0.24	54	9.4		1.52	0.73	3.10	1.040	0.900	0.26
500B-3-1, 79-88	30	70		0.15		4	1.6		0.98	0.58	1.52	0.052	0.040	

Note: NA = neutron activation analyses; XRF = X-ray fluorescence analyses.

fresh basalt to several tens of ppm for altered samples. Considering fresh oceanic basalts on the basis of thin-section observations and ignition loss at 110°C and 1050°C—which can be “negative” at 1050°C because of the uptake of oxygen by Fe⁺⁺ oxidation—the contamination by seawater can more than double the Rb content and increase the Cs content by a factor of 10 (Bougault et al., 1979).

A brief look at alkali-metals data from Legs 66 and 67 (Rb and Cs, Table 12; K₂O, Tables 1, 2, 3) shows a correlation among these alkali elements. This correlation is enhanced in a plot of Cs versus Rb (Fig. 4). In addition, a very good positive correlation is observed between the content of alkali elements and the ignition loss at 1050°C (see Table 12 for Rb and Cs and Tables 1, 2, and 3 for K₂O and loss on ignition). This positive correlation (alkali content and ignition loss), which accounts for the intensity of alteration, is in agreement with the effect of seawater at low temperature mentioned earlier. Nevertheless, two exceptions to this alkali-ignition-loss relationship are observed: the two samples from Core 1, Section 1 of Hole 499C.

Drastic chemical transformations are predicted from laboratory studies of seawater-basalt interactions at high

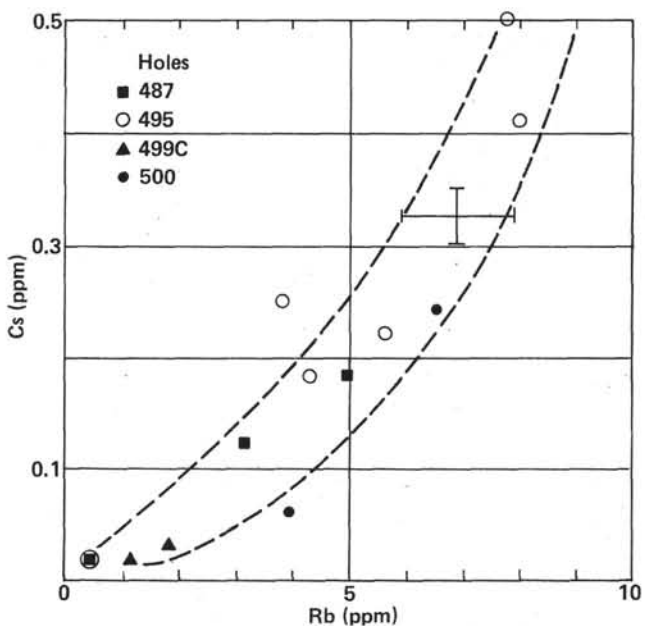


Figure 4. Cs (ppm) versus Rb (ppm) (the correlation between alkali metals for altered samples).

temperatures and at seafloor pressures (Bischoff and Dickson, 1975; Hajash, 1975; Mottl and Holland, 1978). At mid-ocean ridges, temperatures of up to 380°C have been measured, sulfides are precipitated at the mouths of springs, and elements are removed from seawaters and from basalt. (Corliss et al., 1978; Corliss et al., 1979; Francheteau et al., 1979; Rise Project Group, 1980; and J. Honnorez et al., personal communication, 1981). Both experimental data and field observations indicate that alkali metals, Ca (Menzies and Seyfried, 1979; Edmond et al., 1979), and elements such as Mn, Fe, Zn, and Cu (Bischoff and Dickson, 1975; Seyfried and Bischoff, 1977; Hekinian et al., 1980; Boulègue et al., 1980) are leached from the rocks and transported to the seafloor. Alkali metals are then probably diluted in seawater; Mn starts to precipitate according to the rate of its oxidation from Mn^{++} to MnO_2 ; and most of the Fe, Cu, and Zn contents in hydrothermal fluids precipitate as sulphides at the mouth of hot hydrothermal springs on the seafloor or within the conduits to the seafloor, according to the temperature and the input of seawater. Ca has been found to precipitate as sulfate at the mouth of cooler springs. For the two samples from Core 1, Section 1 of Hole 499C the following characteristics are observed:

- 1) The highest loss of volatiles occurs at 110°C and the highest loss on ignition at 1050°C; both results indicate that these samples underwent a strong action of fluids.

- 2) Rb and Cs are low and close to the limit of detection of the analytical techniques; K_2O is in the range of unaltered low K tholeiites. These results preclude a low-temperature seawater alteration leading to alkali enrichments, observed for other samples, and indicate high-temperature basalt-seawater interaction (Edmond et al., 1979; Menzies and Seyfried, 1979).

- 3) Ca is depleted ($CaO \sim 7.2\%$) relative to classical CaO content (12%) found, for instance, in Sample 499D-1-1, 33–35 cm (which does not have the same characteristics of alteration); this fact also points to high-temperature seawater-basalt interaction (Edmond et al., 1979).

- 4) Mn and Zn concentrations are abnormally high, ~2800 ppm and ~360 ppm, compared to classical 1400 ppm and 70 ppm values in tholeiites. Considering the behavior of these elements mentioned earlier, these high concentrations can be interpreted as precipitations of these elements from hydrothermal fluids.

The interpretation that high-temperature seawater-basalt interaction leads to low K, Rb, Cs, and Ca values (the removal of alkali metals from basalt) and to Mn and Zn enrichment by early precipitation from fluids requires that there be no subsequent low-temperature alteration with time. This assumption is possible if we believe that fissures and conduits are quickly filled on the cessation of hydrothermal activity. In addition, we know that it is possible to preserve fresh basalts from seawater alteration for a million years (Donnelly et al., 1980).

High Partition Coefficient and Hygromagnaphile Elements

The concentrations of high partition coefficient elements Cr and Ni in tholeiites vary respectively from 600

ppm (Cr) and 250 ppm (Ni) for primary liquids to 50 ppm (Cr and Ni) for differentiated liquids as crystallization proceeds. During this process Co content remains approximately constant, between 40 and 45 ppm (Bougault, 1977; Bougault et al., 1979). In this respect, it is clear that none of these basalts is "primary" and that all of them can be considered as liquids that have undergone fractional crystallization to different extents.

The Co content in these samples is in agreement with usual tholeiite concentrations except for the two samples from Hole 499C; 29 and 32 ppm are significantly lower than 40 to 45 ppm. We suggest that this observation could be connected with the high-temperature alteration mentioned earlier.

Extended Coryell-Masuda plots present the behavior of hygromagnaphile elements of the Transition Series 1, 2, 3, and 4, those elements whose ions show an electronic structure of rare gas (except V). Such a presentation incorporating non-rare-earth elements within rare earths has already been used to give a general picture of the relative fractionation of elements (e.g., White and Schilling, 1978; Kay et al., 1970; Tarney et al., 1979; Sun et al., 1979; Tarney et al., 1980; Morisson et al., 1980; Sun, 1980). The trends are generally interpreted in terms of primary genesis of rocks. Alkali metals are not used in the figures, because, as already shown, these elements are sensitive to alteration processes. Only the transition elements are used.

Among the data available in the literature, many results concern non-rare-earth elements on the one hand (e.g., Y, Zr, Nb; data are scarcer for the third Transition Series: sometimes Hf and Ta) and rare-earths on the other. Very infrequently are all these elements discussed together for the *same* samples. Until recently, the correct place of non-rare-earths within the rare-earths field was uncertain in the extended Coryell-Masuda plot (which represents the comparative hygromagnaphile-affinity for the liquid phase—character of all of these elements). In addition, the concentration of non-rare-earth elements in chondrites (for normalization) is not known with the required precision. For these reasons the diagrams proposed by Sun et al., (1979), Tarney et al., (1980) and Morisson et al., (1980) are not very precise as far as non-rare-earth elements are concerned.

The data accumulated since the FAMOUS operation and Leg 37, for the *same* powders, allowed us to obtain the following results. (1) The elements of the second and third Transition Series of Groups 3, 4, and 5 (Y/Tb; Zr/Hf; Nb/Ta) do not fractionate one from the other; the ratios are close to the chondritic ratios (Y/Tb = 50; Zr/Hf = 40 [Fig. 5]; Nb/Ta = 16). (2) Normalization values have been computed (Table 13) that are in the range of the proposed concentrations of chondrites in the literature. These values can be handled in the same way as "average rare earth" concentrations in chondrites. (3) The position of non-rare-earth elements within the rare-earths has been precisely determined by comparative geochemistry and also on more theoretical grounds, based on the cumulative effects of the incompatible character of these elements within a mineral structure and the complex formations in liquids (Bougault, 1980). (4) Using results (2) and (3), it is possible to

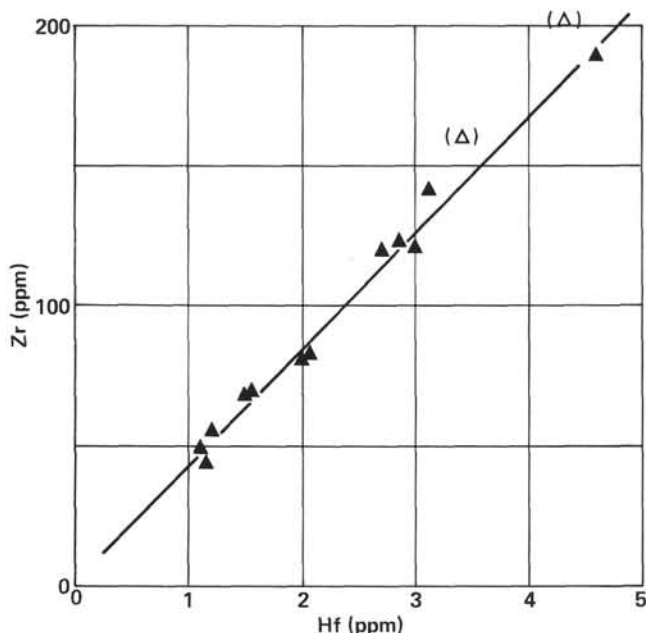


Figure 5. Zr (ppm) versus Hf (ppm) for Legs 66 and 67 samples. (The two open triangles—Samples 495-47-1, 3-8 cm and 500-18-1, 52-54 cm—correspond very probably to an overestimation of Zr, if compared with similar, if not identical, samples from each hole.)

Table 13. Normalization values.

Th	La	Ta	Nb	Zr	Hf	Ti	Eu	Tb	Y	V
0.028	0.32	0.031	0.53	5.13	0.128	460	0.07	0.047	2.16	22

obtain an extended Coryell-Masuda plot including non-rare-earth elements within the rare earths. The logarithm of normalized concentrations of non-rare-earth elements (ordinate) plot in this diagram with the same precision as the rare-earth values themselves. (5) Two values of the normalized Ta/La ratio have been found: 1 and 0.5, which are interpreted to be characteristic of mantle domain. This observation was evident in the papers of Sun et al., (1979) and Tarney et al., (1980) but not mentioned. In the Atlantic, this notion of mantle domain, initially termed "mantle blob" (Schilling, 1975), has been recently confirmed (Bougault and Treuil, 1980) using non-rare-earth elements and has in turn been correlated with isotopic results (Allègre et al., 1980; B. Dupré, personal communication, 1981).

In light of these investigations, what is the information that can be deduced from the present data regarding fundamental and comparative geochemistry, mantle heterogeneity?

A good example of the nonfractionation of the elements of each pair Nb-Ta, Zr-Hf, and Y-Tb is given in Figure 5, where the Zr/Hf ratio is very close to the value 40 found in basalts. The two open triangles correspond to Samples 495-47-1, 3-8 cm and 500-18-1, 53-54 cm and are very probably Zr overestimated by 10 ppm when compared to similar, if not identical, Samples 495-46-1, 138-143 cm and 500-19-1, 24-28 cm, respectively. The

Y/Tb correlation is also very good, but we think that Y has been overestimated by some ppm to account for the systematic upper position of this element relative to Tb in Figures 6 to 11. The Nb/Ta ratio cannot be determined with precision due to low values observed in Holes 487, 495, 499C, 499D, and 500B. Nevertheless, the constancy of this ratio (16) can be estimated from the extended plots where Nb and Ta plot nearly at the same ordinate position. The precision of the extended diagram satisfies the result mentioned earlier—(4)—which also involves results (2) and (3). The plots of the elements lying from Zr to Y in this diagram are demonstrative of that precision, as can be seen by comparing the ordinate positions of non-rare-earth elements to those of rare-earth elements.

Point (5) is very interesting: first of all, the distribution of the hygromagnaphile elements according to an extended Coryell-Masuda plot of Samples from Hole 500 (Fig. 11) is very different from the plots of other holes (Figs. 6-10). The rocks from Holes 487, 495, 499C, 499D, and 500B correspond to classical "depleted" tholeites identical to those drilled during Leg 65 at 21°N on the East Pacific Rise (Cambon et al., in press), and during Leg 54 at 9°N and at the Galapagos spreading center (Joron et al., 1980). On the other hand, the two samples from Hole 500 show a significantly "light-rare-earth" enriched pattern similar to those obtained in the FAMOUS area (Langmuir et al., 1977). Correlatively, for Hole 500, Ta, Nb, and La plot at the same ordinate position, which corresponds to the chondritic normalized Ta/La ratio (= 1, like the FAMOUS area, Bougault and Treuil, 1980; and like the Emperor Seamounts, Cambon et al., 1980); Nb and Ta plot at a lower position than La for all other holes investigated in this study. This feature corresponds to an average normalized Ta/La ratio of about 0.5, as at 21°N and 9°N on the East Pacific Rise, Galapagos Center, and the region of 20°N in the Atlantic (Joron et al., 1980; Bougault and Treuil, 1980). In light of the present interpretation of hygromagnaphile element behavior, we deduce that the Site 500 samples do not derive from the same "mantle domain" as the samples from other sites.

CONCLUSIONS

1. *Typical oceanic crust.* The occurrence of typical oceanic crust in the Guatemala Trench area is established. All the major mineralogical and geochemical features of oceanic tholeites are preserved in the Trench itself (Hole 500) as well as its immediate vicinity (Site 495).

2. *Heterogeneity.* This crust is heterogeneous. Basalts from Hole 500 differ from the typically depleted oceanic tholeites of Holes 495, 499, and 500B in their enrichment in light REE or equivalent elements in an extended Coryell-Masuda plot and in the "alkalic" tendency of their clinopyroxene mineralogy (salites). These differences mirror disparate chemical characteristics of verre mantle sources. We presently have no pertinent explanation for the coexistence in the same area of both REE-enriched and depleted basalts. So far, such an oc-

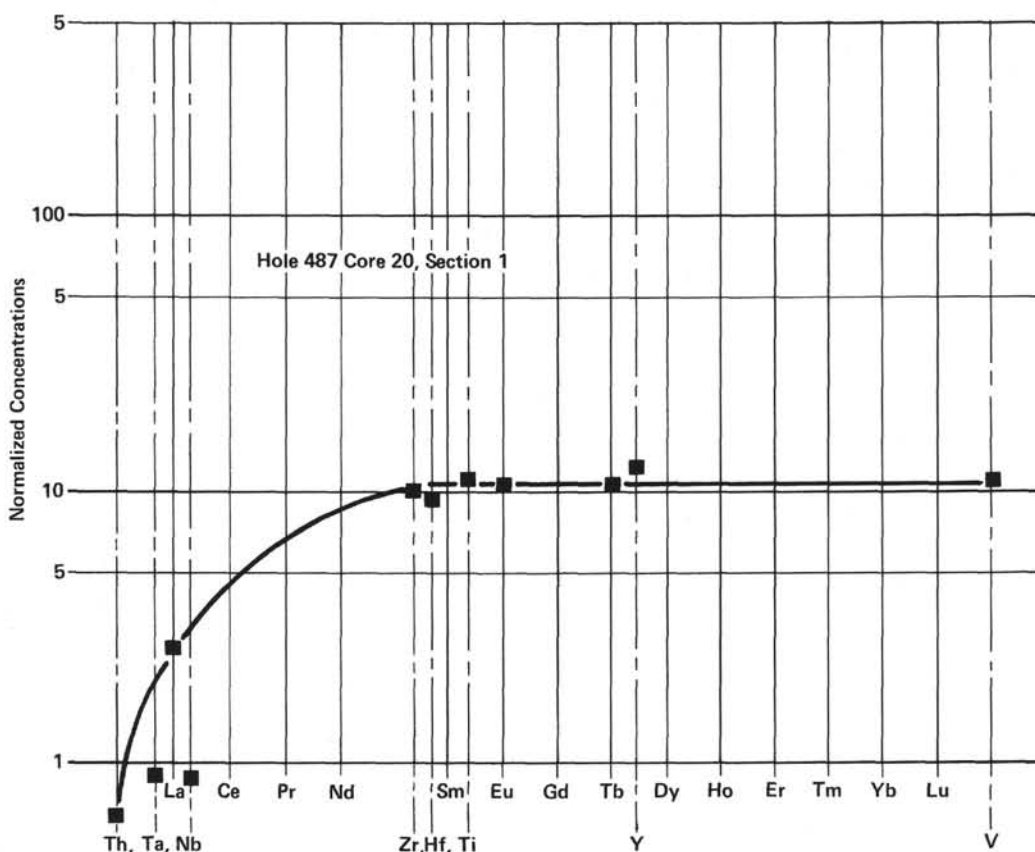


Figure 6. Extended Coryell-Masuda plot, Hole 487. (The sample is from Core 20, Section 1, as indicated).

currence has not been observed either in a given area (e.g., the FAMOUS area, sampling by submersible and dredging) or within a single drilled hole.

3. *Hydrothermalism, metamorphism, and mineralization.* With the exception of Hole 500, volcanic rocks from the Trench (Holes 499B, C, and D; 500D) and from the continental slope (Hole 494A) are characterized by their "spilitic" paragenesis involving mineral associations typical of greenschist facies metamorphism: actinolite + epidote + plagioclase + chlorite + quartz + calcite (Hole 494A); actinolite + plagioclase + chlorite + quartz + calcite (Holes 499B, C, and D; 500-D)—plagioclases ranging in composition from calcic "primary" plagioclase to nearly pure albite. Such metamorphic associations are frequently encountered in spilitic series of orogenic areas considered to be remnants of oceanic crust (e.g., Nicoya series; Azéma and Tournon, this volume) or of orogenic-type magmatism (e.g., Girard and Maury, 1980). They are also commonly found in samples dredged from ocean floors and ridges (e.g., Melson et al., 1968; Miyashiro et al., 1971; Jehl, 1975) and are considered the product of ocean-ridge metamorphism, the origin of which is attributed to hydrothermal (high-temperature) seawater–basalt interactions. The occurrence of actinolite-bearing assemblages in metabasites indicate temperatures higher than 300° to 320°C (Spooner and Fyfe, 1973), and the thermal stability of plagioclase-chlorite-actinolite associations seems to be restricted to a range of 300° to 475°C (Liou and Ernst,

1979). In the present case (Hole 499C), the distribution of alkali metals is satisfactorily explained by such a high-temperature seawater–basalt interaction.

Mineralogical evidence of postmagmatic mineralization, the origin of which can be attributed to hydrothermalism, has been found in samples from Holes 499C (pyrophanite–manganiferous ilmenite) and 500B (manganiferous ilmenite and pyrite). The former samples are characterized by positive anomalies of Mn and Zn contents, probably due to precipitations of these elements from hydrothermal fluids. The geological framework of that hydrothermalism is difficult to elucidate, owing to the reworked character of many samples (Holes 499C and D; 500B). The only metamorphic sample considered to have been drilled from oceanic crust *in situ* is Sample 499B-10-1, 40–46 cm. The occurrence within one area of both fresh and altered oceanic crust has already been reported (Legs 51, 52, 53), and it is not surprising if we assume hydrothermal fluids to be circulating along normal faults. The similarity between the greenschist facies metamorphism developed in the oceanic crust and neighboring continental slope volcanics is striking.

4. *Magmatic affinities of Hole 494A lavas.* These samples have undergone important chemical and mineralogical modifications of hydrothermal origin. Thus their primary character is not easy to identify, and the indications presently obtained are somewhat contradictory. Considering the available mineralogical data (clinopyroxene and plagioclase composition), an "active

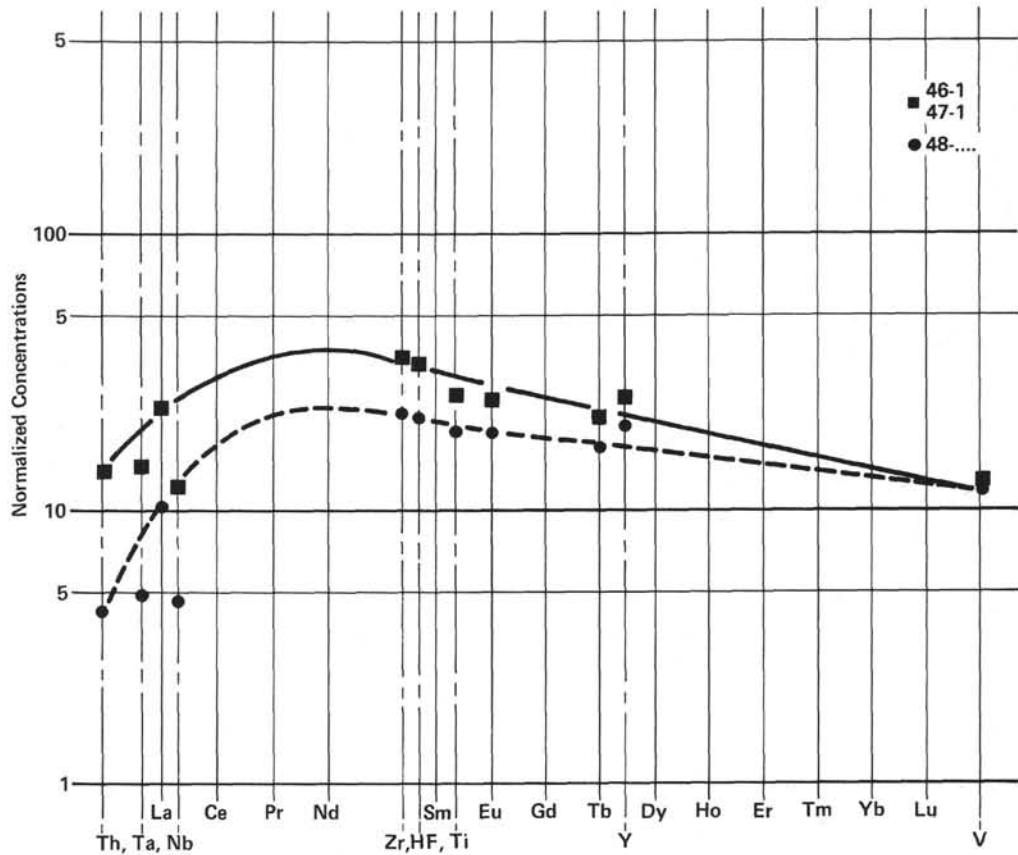


Figure 7. Extended Coryell-Masuda plot, Hole 495. (Cores [e.g., 46] and sections [e.g., 1] are indicated in the legend; for Core 48 [•], the plot corresponds to all analyzed samples of that core.)

margin" affinity is favored, which is also in agreement with the low concentrations of hygromagnaphile elements (Hf, Ti, Eu, Tb; Table 14 and Fig. 12). Nevertheless, the light rare-earth-element-depleted character (or hygromagnaphile equivalent elements) is unusual in orogenic lavas, even if observed for Tongan Island arc tholeiites (Ewart et al., 1973), but it is typical in oceanic tholeiites.

REFERENCES

- Allègre, C. J., Brevart, O., Dupré, B., and Minster, J. F., 1980. Isotopic and chemical effects produced in a continuously differentiating convecting earth mantle. *Philos. Trans. R. Soc. London, Ser. A*, 297:447-477.
- Aubouin, J., von Huene, R., and Leg 67 Scientific Team, 1979. Premiers résultats des forages profonds dans le Pacifique au niveau de la fosse du Guatemala (fosse d'Amérique Centrale) (Leg 67 du "Deep Sea Drilling Project": Mai-Juin 1979). *C. R. Acad. Sci. Paris, Ser. D*, 289:1215-1220.
- Bischoff, J. L., and Dickson, F. W., 1975. Seawater-basalt interactions at 200°C and 500 bars: implications for the origin of sea-floor heavy metal deposits and regulation of seawater chemistry. *Earth Planet. Sci. Lett.*, 25:385-397.
- Bougault, H., 1977. Evidence de la cristallisation fractionnée au niveau d'une ride medio-oceanique: Co, Ni, Cr, FAMOUS, Leg 37 du D.S.D.P. *Bull. Soc. Geol. Fr.*, (7) XIX:1207-1212.
- , 1980. Contribution des éléments de transition à la compréhension de la genèse des basaltes océaniques. Analyse des éléments traces dans les roches par spectrométrie de fluorescence X [*thèse*]. Université de Paris VII.
- Bougault, H., Cambon, P., Corre, O., Joron, J. L., and Treuil, M., 1980. Evidence for variability of magmatic processes and upper mantle heterogeneity in the axial region of the Mid-Atlantic Ridge near 22°N and 36°N. *Tectonophysics*, 55:11-34.
- Bougault, H., Cambon, P., and Toulhost, H., 1977. X-ray spectrometric analysis of trace elements in rocks. Correction for instrumental interferences. *X-Ray Spectrom.*, 6:66-72.
- Bougault, H., Joron, J. L., and Treuil, M., 1979. Alteration, fractional crystallization, partial melting, mantle properties from trace elements in basalts recovered in the North Atlantic. In Talwani, M., Harrison, C. G., and Hayes, D. E. (Eds.), *Deep Drilling Results in the Atlantic Ocean: Ocean Crust: Maurice Ewing Series* (Vol. 2), (A.G.U.), 352-368.
- Bougault, H., Maury, R. C., El Azzouzi, M., Joron, J. L., Cotten, J., and Treuil, M., 1982. Tholeiites, basaltic andesites and andesites from Leg 60 sites: Geochemistry, mineralogy and low partition coefficient elements. In Husson, D., Uyeda, S., et al., *Init. Repts. DSDP*, 60: Washington (U.S. Govt. Printing Office), 657-678.
- Bougault, H., and Treuil, M., 1980. Mid-Atlantic Ridge: zero-age geochemical variations between Azores and 22°N. *Nature*, 286 (5770):209-212.
- Boulègue, J., Michard, G., Bougault, H., and Charlou, J. L., 1980. Hydrothermal activity in the East Pacific Rise between 15°N and 7°S. *Eos*, 61:992.
- Brousse, R., Maury, R. C., in press. Titaniferous basanites and hawaiites from Mehetia, Society Islands, Central Pacific.
- Cambon, P., Joron, J. L., Bougault, H., and Treuil, M., 1980. Leg 55 Emperor seamounts: trace elements in transitional tholeiites, alkali basalts, and hawaiites—mantle homogeneity or heterogeneity and magmatic processes. In Jackson, E. D., Koizumi, I., et al., *Init. Repts. DSDP*, 55: Washington (U.S. Govt. Printing Office), 585-597.
- , in press. Leg 65: East Pacific Rise—typical oceanic crust depleted in hygromagnaphile elements. In Lewis, B. T. R., Robinson, P., et al., *Init. Repts. DSDP*, 65: Washington (U.S. Govt. Printing Office).

- Corliss, J. B., Dymond, J., Gordon, L. I., Edmond, J. M., Von Herzen, R. P., Ballard, R. D., Green, K., Williams, D., Bainbridge, A., Crane, K., and van Andel, Tj. H., 1979. Submarine thermal springs on the Galapagos Rift. *Science*, 203:1973-1983.
- Corliss, J. B., Lyle, M., Dymond, J., and Crane, K., 1978. The chemistry of hydrothermal mounds near the Galapagos Rift. *Earth Planet. Sci. Lett.*, 40:12-24.
- Donnelly, T. W., Francheteau, J., Bryan, W., Robinson, P., Flower, M., and Salisbury, M., 1980. *Init. Repts. DSDP*, 51, 52, 53: Washington (U.S. Govt. Printing Office).
- Donnelly, T. W., Thompson, G., and Robinson, P. T., 1979. Very low-temperature hydrothermal alteration of the oceanic crust and the problem of fluxes of potassium and magnesium. In Talwani, M., Harrison, C. G., and Hayle, D. E. (Eds.), *Deep Drilling Results in the Atlantic Ocean: Ocean Crust: Maurice Ewing Series* (Vol. 2), (A.G.U.), 369-382.
- Edmond, J. M., Corliss, J. B., and Gordon, L. I., 1979. Ridge crest: hydrothermal metamorphism at the Galapagos spreading center and reverse weathering. In Talwani, M., Harrison, C. G., and Hayle, D. E. (Eds.), *Deep Drilling Results in the Atlantic Ocean: Ocean Crust: Maurice Ewing Series* (Vol. 2), (A.G.U.), 383-390.
- Ewart, A., Bryan, W. B., and Gill, J. B., 1973. Mineralogy and geochemistry of the younger volcanic islands of Tonga, SW Pacific. *J. Petrol.*, 14:429-465.
- Francheteau, J., Needham, H. D., Choukroune, P., Juteau, T., Seguret, M., Ballard, R. D., Fox, P. J., Nordmark, W., Carranza, A., Cordoba, D., Guerrero, J., Rangin, C., Bougault, H., Cambon, P., and Hekinian, R., 1979. Massive deep-sea sulphide ore deposits discovered on the East Pacific Rise. *Nature*, 277(Wo 5697):523-528.
- Galli-Olivier, C., 1979. Ophiolite and island-arc volcanism in Costa Rica. *Geol. Soc. Am. Bull.*, 90:444-452.
- Girard, D., and Maury, R. C., 1980. Affinité tholeiitique d'arc insulaire des spilites de l'île de Tobago (Petites Antilles). *C. R. Acad. Sci. Paris, Ser. D*, 290:935-938.
- Hajash, A., 1975. Hydrothermal processes along mid-ocean ridges. An experimental investigation. *Contrib. Mineral. Petrol.*, 75:1-13.
- Hart, S., 1969. K, Rb, Cs contents and K/Rb, K/Cs ratios of fresh and altered submarine basalts. *Earth Planet. Sci. Lett.*, 6: 295-303.
- Hawkins, Sr., J. W., 1977. Petrologic and geochemical characteristics of marginal basin basalts. In Talwani M., and Pitman, III, W. C. (Eds.), *Island Arcs Deep-sea Trenches, and Back-arc Basins: Maurice Ewing Series* (Vol. 1), (A.G.U.), 355-366.
- Hekinian, R., Fevrier, M., Bischoff, J. L., Picot, P., and Shanks, W. C., 1980. Sulphide deposits from the East Pacific Rise near 21°N. *Science*, 207:1433-1444.
- Jaffrezic, H., Joron, J. L., and Treuil, M., 1977. Trace elements determination in rock powder. A study of the precision for a given analytical procedure. Instrumental epithermal neutron activation. *J. Radioanal. Chem.*, 39:185-188.
- Jehl, V., 1975. Le métamorphisme et les fluides associés des roches océaniques de l'Atlantique Nord [these]. Université de Nancy.
- Joron, J. L., Bollinger, C., Quisefit, J. P., Bougault, H., and Treuil, M., 1980. Trace elements in Cretaceous basalts at 25°N in the Atlantic Ocean: alteration, mantle compositions, and magmatic processes. In Robinson, P., Flower, M., and Salisbury, M., et al., *Init. Repts. DSDP*, 51, 52, 53, Pt. 2: Washington (U.S. Govt. Printing Office), 1087-1098.
- Joron, J. L., Bougault, M., Maury, R. C., and Stephan, J. F., 1982. Basalt from the Cocos Plate (Site 487, Leg 66): petrology and geochemistry. In Watkins, J. S., Moore, J. C., et al., *Init. Repts. DSDP*, 66: Washington (U.S. Govt. Printing Office), 731-736.
- Joron, J. L., Briquet, L., Bougault, H., and Treuil, M., 1980. East Pacific Rise Galapagos spreading center and Siqueiros fracture zone, Deep Sea Drilling Project Leg 54: hygromagnaphile elements. A comparison with the North Atlantic. In Rosendahl, B. R., Hekinian, R., et al., *Init. Repts. DSDP*, 54: Washington (U.S. Govt. Printing Office), 725-735.
- Kay, R., Hubbard, N. J., and Gast, P. W., 1970. Chemical characteristics and origin of oceanic ridge volcanic rocks. *J. Geophys. Res.*, 73:1585-1613.
- Konda, T., 1970. Endiopside in the calc-alkaline basalt in the Ryozen area. *J. Geol. Soc. Jpn.*, 76:7-12.
- Langmuir, C. H., Bender, J. F., Bence, A. E., Hanson, G. N., and Taylor, S. R., 1977. Petrogenesis of basalts from the FAMOUS area: Mid-Atlantic Ridge. *Earth Planet. Sci. Lett.*, 36:133-156.
- Leake, B. E., 1978. Nomenclature of amphiboles. *Bull. Mineral.*, 101: 453-467.
- Le Guen de Kerneizon, M., Mascole, A., Maury, R. C., and Westercamp, D., 1979. Les laves de la Desirade (Petites Antilles), témoins d'un magmatisme de marge active: arguments mineralogiques. *Bull. Bur. Rech. Geol. Min. Sect. 4*, 314:285-292.
- Liou, J. G., and Ernst, W. G., 1979. Ocean ridge metamorphism of the East Taiwan ophiolite. *Contrib. Mineral. Petrol.*, 68:335-348.
- Marcelot, G., 1980. Contribution à l'étude du volcanisme des Nouvelles-Hebrides: petrographie, mineralogie et géochimie des laves d'Errmango [these]. Université de Paris XI.
- Maury, R. C., Brousse, R., Villemant, B., Joron, J. L., Jaffrezic, H., and Treuil, M., 1980. Cristallisation fractionnée d'un magma basaltique alcalin: la série de la Chaîne des Puys (Massif Central, France). I. *Petrologie Bull. Mineral.*, 103:250-266.
- Melson, W. G., Thompson, G., and van Andel, Tj. H., 1968. Volcanism and metamorphism in the Mid-Atlantic Ridge, 22°N latitude. *J. Geophys. Res.*, 73:5295-5941.
- Menzies, M., and Seyfried, W. E., Sr., 1979. Basalt-seawater interaction, trace element and strontium isotopic variations in experimentally altered glassy basalt. *Earth Planet. Sci. Lett.*, 44: 463-472.
- Mevel, C., and Velde, D., 1976. Clinopyroxenes in Mesozoic pillow lavas from the French Alps: influence of cooling rate on compositional trends. *Earth Planet. Sci. Lett.*, 32:158-164.
- Miyashiro, A., Shido, F., and Ewing, M., 1971. Metamorphism in the Mid-Atlantic Ridge near 24° and 30°N. *Philos. Trans. R. Soc. London Ser. A*, 268:589-603.
- Morisson, M. A., Thompson, R. N., Gibson, I. L., and Marriner, G. F., 1980. Lateral chemical heterogeneity in the Palaeocene upper mantle beneath the Scottish Hebrides. *Philos. Trans. R. Soc. London Ser. A*, 297:229-244.
- Mottl, M. J., and Holland, H. D., 1978. Chemical exchange during hydrothermal alteration of basalt by seawater. I. Experimental results for major and minor components of seawater. *Geochim. Cosmochim. Acta*, 42:1103-1115.
- Rise Project Group, 1980. East Pacific Rise: hot springs and geophysical experiments. *Science*, 207:1421-1433.
- Schilling, J. G., 1975. Rare earth variations across "normal segments" of the Reykjanes Ridge, 60°-53°N, Mid-Atlantic Ridge, 29°S, and East Pacific Rise, 2°-19°S, and evidence on the composition of the underlying low-velocity layer. *J. Geophys. Res.*, 80:1459-1473.
- Schweitzer, E. L., Papike, J. J., and Bence, E. A., 1979. Statistical analysis of clinopyroxenes from deep-sea basalts. *Am. Mineral.*, 64:501-513.
- Seyfried, W., and Bischoff, J. L., 1977. Hydrothermal transport of heavy metals by seawater: the role of seawater/basalt ratio. *Earth Planet. Sci. Lett.*, 34:71-77.
- Sigurdsson, H., and Schilling, J. G., 1976. Spinels in Mid-Atlantic Ridge basalts: chemistry and occurrence. *Earth Planet. Sci. Lett.*, 29:7-20.
- Smith, D., and Lindsley, D. H., 1971. Stable and metastable augite crystallization trends in a single basalt flow. *Am. Mineral.*, 56: 225-233.
- Spooner, E. T. C., and Fyfe, W. S., 1973. Sub-sea-floor metamorphism, heat and mass transfer. *Contrib. Mineral. Petrol.*, 42: 287-304.
- Sun, S. S., 1980. Lead isotopic study of young volcanic rocks from mid-ocean ridges, ocean islands, and island arcs. *Philos. Trans. R. Soc. London Ser. A*, 297:409-445.
- Sun, S. S., Nesbitt, R. W., and Sharaskin, A. Y., 1979. Geochemical characteristics of mid-ocean ridge basalts. *Earth Planet. Sci. Lett.*, 44:119-138.
- Tarney, J., Wood, D. A., Saunders, A. D., Cann, J. R., and Varet, J., 1980. Nature of mantle heterogeneity in the North Atlantic: evidence from deep sea drilling. *Philos. Trans. R. Soc. London Ser. A*, 297:179-202.
- Tarney, J., Wood, D. A., Varet, J., Saunders, A. D., and Cann, J. R., 1979. Nature of mantle heterogeneity in the North Atlantic: evidence from Leg 49 basalts. In Talwani, M., Harrison, C. G.,

- and Hayes, D. E. (Eds.), *Deep Drilling Results in the Atlantic Ocean: Ocean Crust: Maurice Ewing Series* (Vol. 2), (A.G.U.), 285–301.
- Tracy, R. I., and Robinson, P., 1977. Zoned titanian augite in alkali olivine basalts from Tahiti and the nature of titanium substitutions in augite. *Am. Mineral.*, 62:634–645.
- White, W., and Schilling, J. G., 1978. The nature and origin of geochemical variation in Mid-Atlantic Ridge basalts from the central North Atlantic. *Geochim. Cosmochim. Acta*, 42:1501–1516.
- Wood, D. A., Tarney, J., Varet, J., Saunders, A. A., Bougault, H., Joron, J. L., Treuil, M., and Cann, J., 1979. Geochemistry of basalts drilled in the North Atlantic by IPOD Leg 49: implications for mantle heterogeneity. *Earth Planet. Sci. Lett.*, 42:77–97.

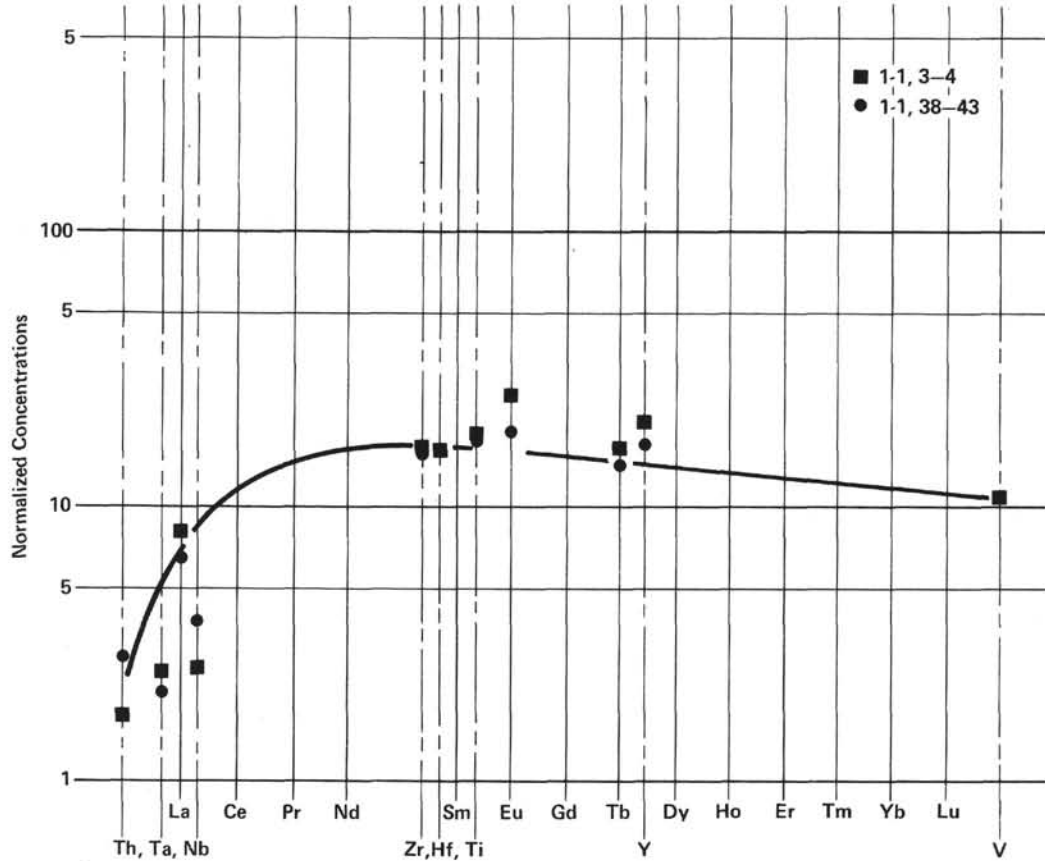


Figure 8. Extended Coryell-Masuda plot, Hole 499C. (Core-section, and interval in cm are indicated in the legend.)

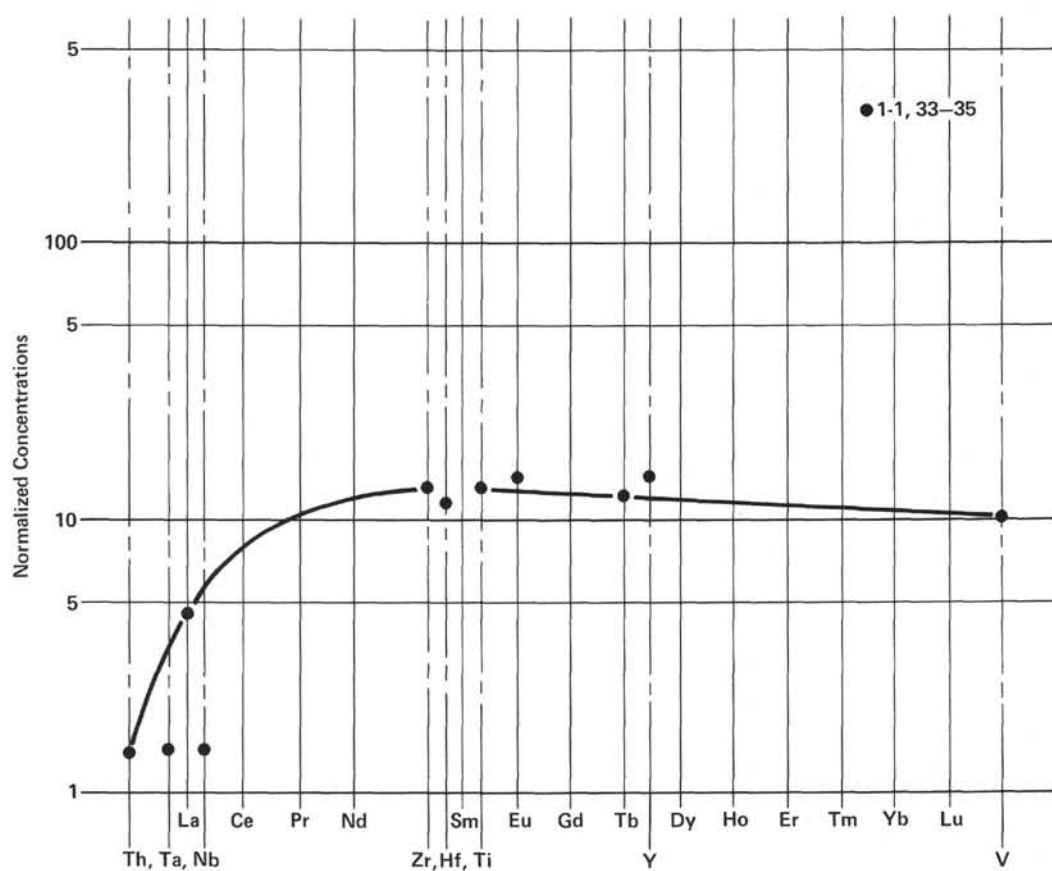


Figure 9. Extended Coryell-Masuda plot, Hole 499D. (Core-section, and interval in cm appear in legend.)

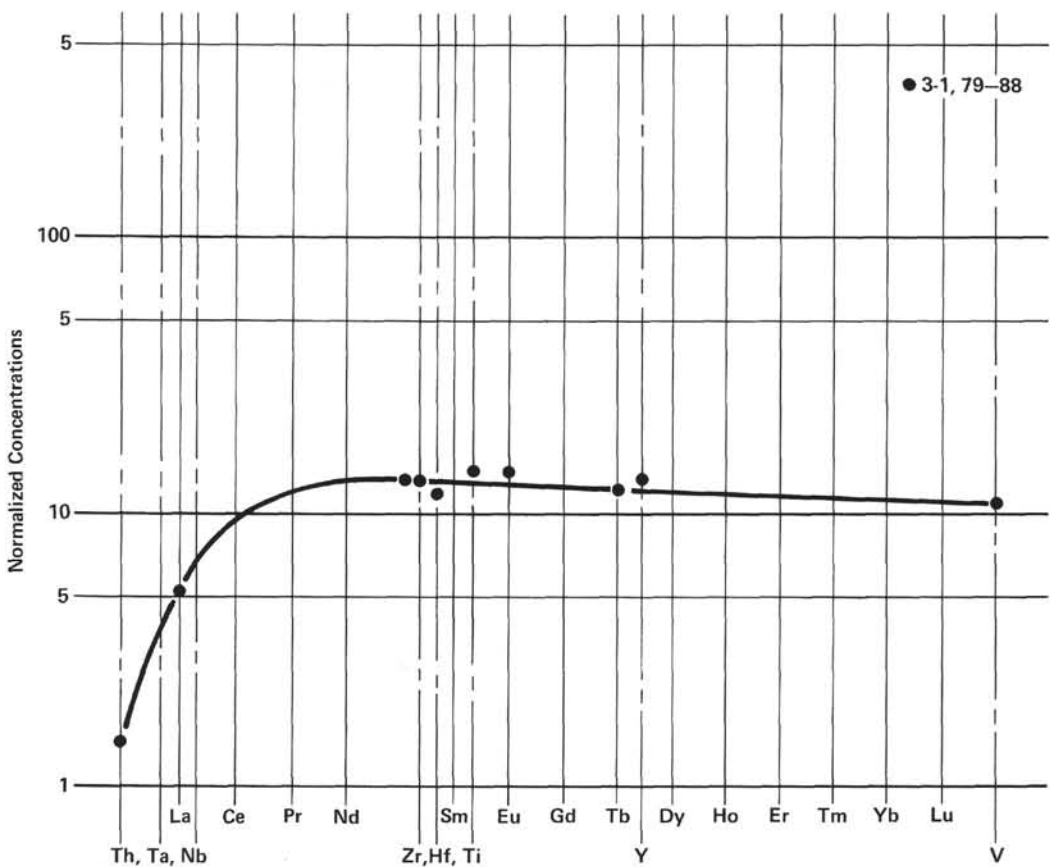


Figure 10. Extended Coryell-Masuda plot, Hole 500B. (Core-section, and interval in cm are noted.)

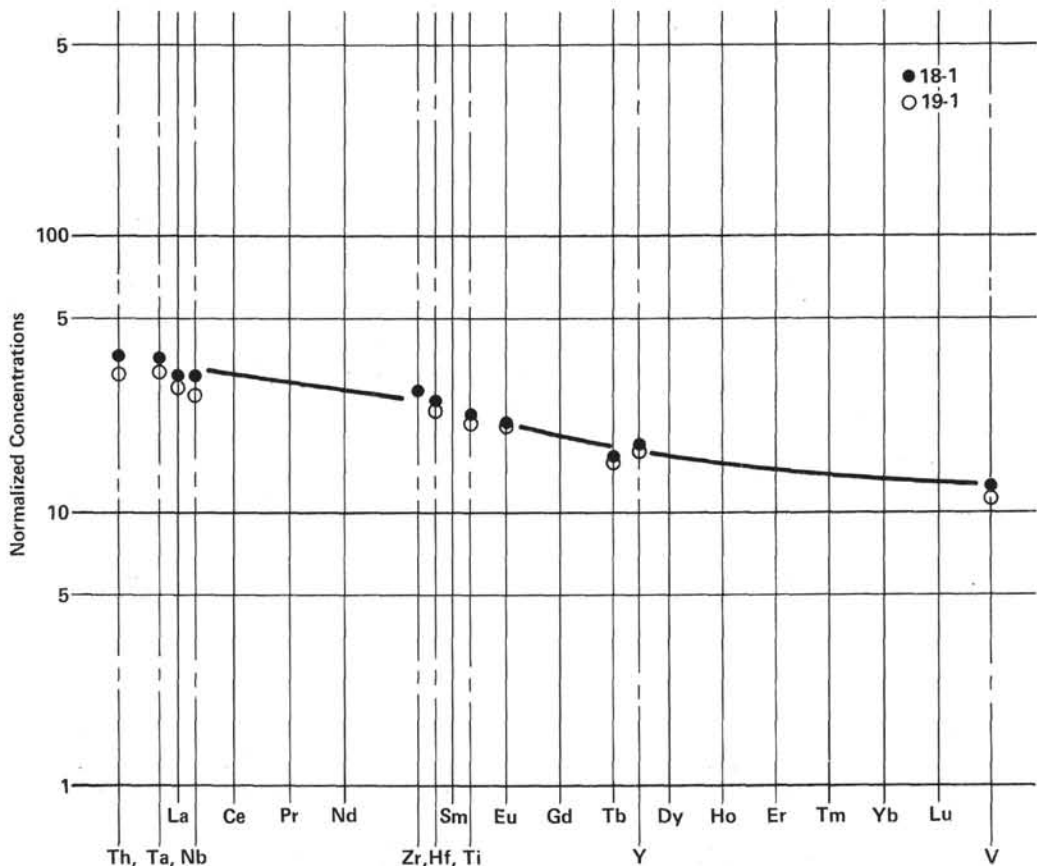


Figure 11. Extended Coryell-Masuda plot, Hole 500. (Cores and sections are indicated.)

Table 14. Trace elements analyses (ppm) of Hole 494A samples.

Sample (interval in cm)	Trace Elements (ppm)																				
	Sc (NA)	Ti (NA)	V (XRF)	Cr (XRF)	Mn (XRF)	Fe (XRF)	Co (XRF)	Ni (XRF)	Zn (XRF)	Rb (XRF)	Sr (XRF)	Y (XRF)	Zr (XRF)	Nb (XRF)	Sb (NA)	Cs (NA)	La (NA)	Eu (NA)	Tb (NA)		
494A-29,CC (0-4)	36.5	2100			1080	56350	36	78						0.03	0.07	0.41	0.27	0.2			
494A-33,CC (18-20)	30.3	3000	250	17	2090	68250	36	34.5	38	36	107	1.7	107	16.7	37	2.7	0.10	0.03	0.47	0.44	0.28
494A-33,CC (30-32)	29.5	2460	138	144	930	53970	31	32.3	68	75	56	2.9	75	11.6	37	0.3	0.03	0.41	0.24	0.19	
494A-35,CC (8-10)	34.1	3060	234	203	1240	59780	35	35.7	87	94	65	1.9	88	16.1	33	2.5	0.02	0.01	0.98	0.53	0.28

Note: NA = neutron activation analyses; XRF = X-ray fluorescence analyses.

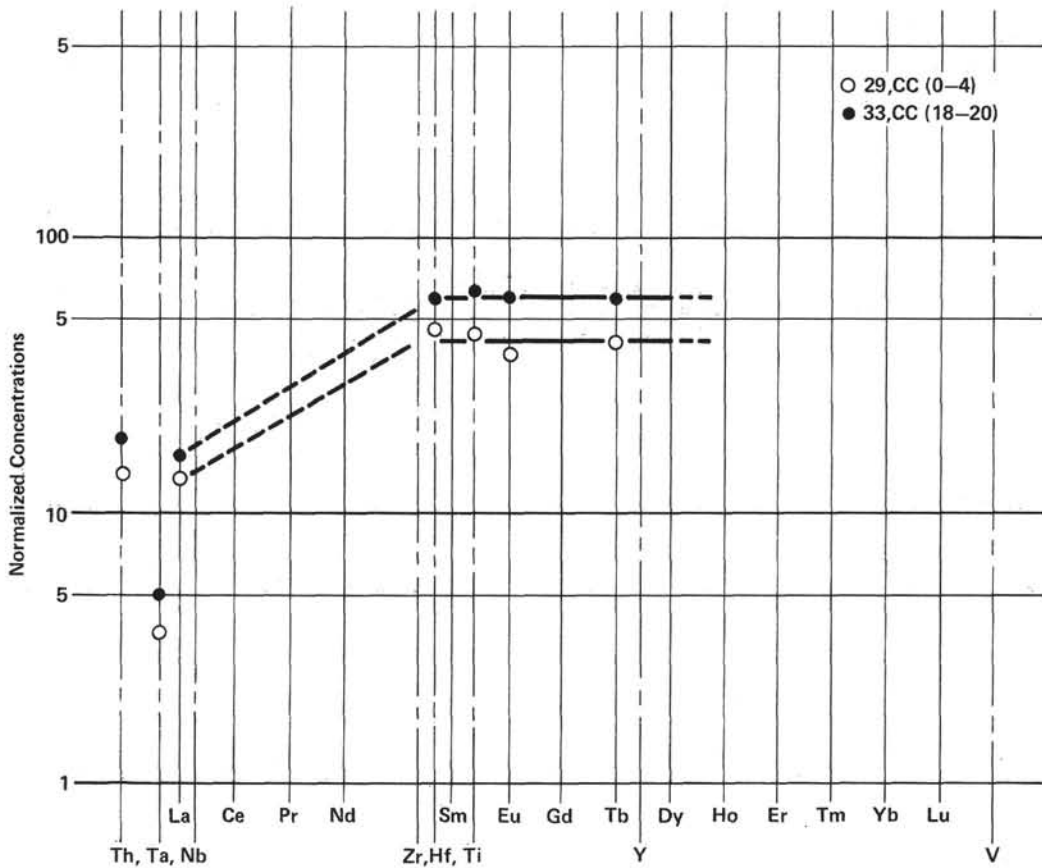


Figure 12. Extended Coryell-Masuda plot, Hole 494A. (Core-catcher sample and interval in cm are indicated.)